

# The $1:\sqrt{2}$ mode interaction and heteroclinic networks in Boussinesq convection

Olga Podvigina<sup>a,b,c,\*</sup>, Peter Ashwin<sup>d</sup>

<sup>a</sup> *Observatoire de la Côte d'Azur, CNRS UMR 6529, BP 4229, 06304 Nice Cedex 4, France*

<sup>b</sup> *International Institute of Earthquake Prediction Theory and Mathematical Geophysics, 79 bldg. 2, Warshavskoe Ave., 113556 Moscow, Russian Federation*

<sup>c</sup> *Laboratory of General Aerodynamics, Institute of Mechanics, Lomonosov Moscow State University, 1, Michurinsky Ave., 119899 Moscow, Russian Federation*

<sup>d</sup> *Mathematics Research Institute, University of Exeter, Exeter EX4 4QE, UK*

Received 20 February 2007; received in revised form 26 June 2007; accepted 28 June 2007

Available online 1 July 2007

Communicated by B. Sandstede

## Abstract

Methods of equivariant bifurcation theory are applied to Boussinesq convection in a plane layer with stress-free horizontal boundaries and an imposed square lattice periodicity in the horizontal directions. We consider the problem near the onset of instability of the uniform conducting state where spatial roll patterns with two different wavelengths in the ratio  $1:\sqrt{2}$  become simultaneously unstable at a mode interaction. Center manifold reduction yields a normal form on  $\mathbb{C}^4$  with very rich dynamical behavior. For a fixed Prandtl number  $P$  the mode interaction occurs at an isolated point in the parameter plane  $(R, L)$  (where  $R$  is the Rayleigh number and  $L$  the length of the horizontal periodicities) and acts as an organizing center for many nearby bifurcations. The normal form predicts the appearance of many steady states and travelling waves, which are classified by their symmetries. It also predicts the appearance of robust heteroclinic networks involving steady states with several different symmetries, and robust attractors of generalized heteroclinic type that include connections from equilibria to subcycles. This is the first example of a heteroclinic network in a fluid dynamical system that has ‘depth’ greater than one. The normal form dynamics is in good correspondence (both quantitatively and qualitatively) with direct numerical simulations of the full convection equations.

© 2007 Elsevier B.V. All rights reserved.

*Keywords:* Mode interaction; Steady state bifurcation with symmetry; Center manifold reduction; Boussinesq convection; Robust heteroclinic network

## 1. Introduction

Thermal convection, a common and important phenomenon in nature, has been a subject of intensive scientific investigation for more than a century. It was investigated by a variety of analytical (asymptotic, perturbation, multiscale, etc.) and numerical methods, as well as by experimental work. Convection is a source of new ideas, for example, on pattern formation and on transition from order to chaos and from laminar to turbulent flows.

In this paper we consider fluid in a non-rotating plane horizontal layer heated from below, assuming the Boussinesq approximation, whereby variation of density is neglected in the mass conservation equation and flows are regarded as incompressible. For small Rayleigh number,  $R$  (proportional to the temperature difference between the horizontal boundaries), fluid is at rest and heat is transferred by thermal diffusion only. When  $R$  exceeds the critical value, fluid motion in the form of two-dimensional rolls sets in. We assume periodicity in horizontal directions with equal periods, such that instabilities with respect to rolls aligned along edges and along diagonals of the periodicity cell occur simultaneously (for the same value of  $R$ ). Spatial periods of these critical modes are in the ratio  $1:\sqrt{2}$ .

\* Corresponding address: International Institute of Earthquake Prediction Theory and Mathematical Geophysics, Laboratory of Nonlinear Dynamics, 79 bldg. 2, Warshavskoe Ave., 117556 Moscow, Russian Federation. Tel.: +7 095 9775195; fax: +7 095 3107032.

E-mail address: [olgap@mitp.ru](mailto:olgap@mitp.ru) (O. Podvigina).

For a square periodicity cell the symmetry group of the system is  $\mathbf{D}_4 \times \mathbf{T}^2 \times \mathbf{Z}_2$  and the center eigenspace is  $\mathbf{C}^4$ . We derive a general third-order ODE (a normal form) commuting with the action of the group on the center eigenspace, and study its bifurcations. The system has a large variety of steady states and travelling waves, which are classified by their symmetries. It can also possess heteroclinic connections forming complex networks. We derive sufficient conditions for existence of some of these connections.

Steady states emerging in a  $\mathbf{D}_4 \times \mathbf{T}^2 \times \mathbf{Z}_2$ -symmetric system on  $\mathbf{C}^2$  have been considered by a number of authors; notably [22,19,20], and bifurcations in a  $\mathbf{D}_4 \times \mathbf{T}^2$ -symmetric system (to which equations of non-Boussinesq convection are reduced) involving  $1:\sqrt{2}$  mode interaction were studied in [18]. The Boussinesq case is richer; in particular, it gives rise to more steady states than are found in [18]. We note that a number of other authors (e.g., [6,5,19,20]) have considered related bifurcations of platforms for periodic boundary conditions on a square lattice.

We apply our results on bifurcations in the general normal form to the particular case of Boussinesq convection, considering the normal form for the values of coefficients calculated by the center manifold reduction of the equations of convection. We obtain bifurcation diagrams of the behavior near the mode interaction in terms of three parameters that generically unfold the problem, which are the Rayleigh number  $R$ , the domain size  $L$  and the Prandtl number  $P$ . We study attractors of the reduced system when the growth rates of roll modes (depending on  $R$  and  $L$ ) are varied and  $P$  is fixed. This study was performed for several values of Prandtl number, and we usually vary  $k = 2\pi/L$  and  $R$  rather than  $L$  directly.

In addition to steady states and periodic orbits, the system possesses several types of heteroclinic attractor, as well as robust heteroclinic-type attractors incorporating connections between equilibria and subcycles. The latter are heteroclinic networks of ‘depth 2’ in the terminology of [1], because there are trajectories within the attractor that connect unstable equilibria and heteroclinic cycles of the more conventional type. More precisely, there are connections that do not lie within the stable manifold of any relative equilibrium. Although such attractors have been found in other systems (e.g., replicator systems [3]) this is the first example in a dynamical system related to hydrodynamics.

Bifurcations of the normal form are compared with those observed in numerical simulations of equations of convection. Attractors in the systems are similar, and the critical values of parameters agree well.

## 2. Thermal convection in a plane layer

Consider the nondimensional equations for Boussinesq convection of a unit density fluid in a plane layer  $(x, y, z)$  (where  $0 < z < 1$ ) uniformly heated from below. The flow velocity  $\mathbf{v}$  and pressure  $p$  satisfy the Navier–Stokes equation

$$\frac{\partial \mathbf{v}}{\partial t} = \mathbf{v} \times (\nabla \times \mathbf{v}) + P \Delta \mathbf{v} + PR\theta \mathbf{e}_z - \nabla p \quad (1)$$

with incompressibility condition

$$\nabla \cdot \mathbf{v} = 0. \quad (2)$$

The heat transfer equation

$$\frac{\partial \theta}{\partial t} = -(\mathbf{v} \cdot \nabla)\theta + v_z + \Delta \theta \quad (3)$$

gives the evolution of  $\theta$ , the difference between the temperature in the flow and the linear temperature profile. The parameters  $R$  and  $P$  are the Rayleigh and Prandtl numbers, respectively. We assume stress-free boundary conditions for the flow and fixed temperature on horizontal boundaries:

$$\frac{\partial v_x}{\partial z} = \frac{\partial v_y}{\partial z} = v_z = 0, \quad \theta = 0 \text{ at } z = 0, 1. \quad (4)$$

For the remainder of the paper we will consider only those flows that are periodic on a square lattice in the  $(x, y)$  plane, i.e. such that there is an  $L > 0$  such that

$$\mathbf{v}(x, y, z) = \mathbf{v}(x + pL, y + qL, z) \quad \text{and} \quad \theta(x, y, z) = \theta(x + pL, y + qL, z) \quad (5)$$

for any  $(p, q) \in \mathbf{Z}^2$ .

The system (1)–(4) admits the trivial solution  $\mathbf{v} = 0, \theta = 0$  describing pure thermal conduction. The steady state becomes unstable to perturbations with wavenumber  $k$  at  $R = (k^2 + \pi^2)^3 k^{-2}$  with an associated eigenvector

$$\mathbf{V}(k) = \begin{pmatrix} -\pi k^{-1} \cos \pi z \sin kx \\ 0 \\ \sin \pi z \cos kx \\ (k^2 + \pi^2)^{-1} \sin \pi z \cos kx \end{pmatrix}. \quad (6)$$

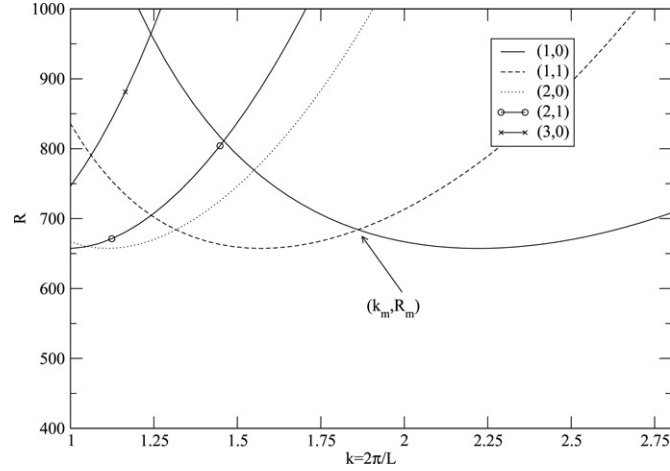


Fig. 1. Critical Rayleigh number  $R$  as a function of  $k = 2\pi/L$  for a range of modes in a box with horizontal dimension  $L$ . The line  $(p, q)$  indicates where the trivial steady state  $\mathbf{v} = \mathbf{0}$  becomes unstable to the mode with wavevector  $(pk, qk, \pi)$ ; there are additional lines for lower  $k$  and higher  $p^2 + q^2$  that accumulate on  $k = 0$ . The point  $(k_m, R_m)$  shows where the  $1:\sqrt{2}$  mode interaction occurs.

(Other eigenvectors can be obtained by application of symmetries of the system.) The critical Rayleigh number for the onset of convection is  $R = \frac{27}{4}\pi^4 \approx 657$ , and the critical wavenumber is  $k_c = \pi/\sqrt{2}$ . Fig. 1 shows the instability neutral curves for the first few modes in the  $(k, R)$  plane.

Modes with wavenumbers  $k$  and  $\sqrt{2}k$  become unstable simultaneously at

$$R_m = 2^{-2/3}(2^{1/3} + 1)^{-2}(2^{2/3} + 2^{1/3} + 1)^3\pi^4 \approx 684 \quad (7)$$

while the critical wavenumber for the mode interaction point satisfies

$$k_m = 2^{-1/6}(2^{1/3} + 1)^{-1/2}\pi \approx 1.86 \quad (8)$$

in agreement with the value reported in [18]. The periodicity  $L$  in Eq. (5) is chosen to be close to the critical value

$$L_m = 2\pi/k_m = 2 \cdot 2^{1/6}(2^{1/3} + 1)^{1/2} \quad (9)$$

so that the rolls  $\mathbf{V}(k_m)$  are aligned along the edges of the periodicity cell. The rolls

$$\mathbf{W}(k_m) = \begin{pmatrix} -\pi k_m^{-1} \cos \pi z \sin(k_m x + k_m y) \\ -\pi k_m^{-1} \cos \pi z \sin(k_m x + k_m y) \\ \sin \pi z \cos(k_m x + k_m y) \\ (2k_m^2 + \pi^2)^{-1} \sin \pi z \cos(k_m x + k_m y) \end{pmatrix} \quad (10)$$

with the wavenumber  $\sqrt{2}k_m$  are aligned along a diagonal.

### 2.1. The symmetry group

The symmetry group of the convective system (1)–(3) with the boundary conditions Eqs. (4) and (5) can be expressed as  $\mathbf{D}_4 \times \mathbf{T}^2 \times \mathbf{Z}_2$ . The eight-element group of symmetries of the square lattice,  $\mathbf{D}_4$ , is comprised of the set of rotations

$$\begin{aligned} s_1 &: (x, y, z) \mapsto (y, -x, z), \\ s_2 &: (x, y, z) \mapsto (-x, -y, z), \\ s_3 &: (x, y, z) \mapsto (-y, x, z), \end{aligned}$$

reflections

$$\begin{aligned} s_4 &: (x, y, z) \mapsto (x, -y, z), \\ s_5 &: (x, y, z) \mapsto (-x, y, z), \\ s_6 &: (x, y, z) \mapsto (y, x, z), \\ s_7 &: (x, y, z) \mapsto (-y, -x, z) \end{aligned}$$

and the identity  $s_0 = e$ . The group  $\mathbf{T}^2 = \mathbf{T}_x \times \mathbf{T}_y$  where  $\mathbf{T}_x$  and  $\mathbf{T}_y$  are groups of translations in the  $x$  and  $y$  directions, respectively:

$$\gamma_\alpha^x : (x, y, z) \mapsto (x + \alpha, y, z)$$

and

$$\gamma_\alpha^y : (x, y, z) \mapsto (x, y + \alpha, z)$$

where  $0 \leq \alpha < L$  (so that  $\gamma_L^x = \gamma_L^y = e$ ). Denote by  $\mathbf{T}_{xy}$  the group of translations along the diagonal:

$$\gamma_\alpha^{xy} : (x, y, z) \mapsto (x + \alpha, y + \alpha, z).$$

The group  $\mathbf{Z}_2$  is generated by the so-called Boussinesq symmetry, which is reflection about the horizontal mid-plane:

$$r : (x, y, z) \mapsto (x, y, 1 - z).$$

Consider a center eigenspace spanned by rolls (6) and (10) and their symmetric images

$$\begin{aligned} \mathbf{X}_1 &= \mathbf{V}, & \mathbf{Y}_1 &= \gamma_{L/4}^x \mathbf{V}, & \mathbf{X}_2 &= s_6 \mathbf{V}, & \mathbf{Y}_2 &= \gamma_{L/4}^y s_6 \mathbf{V}, \\ \mathbf{X}_3 &= \mathbf{W}, & \mathbf{Y}_3 &= \gamma_{L/4}^x \mathbf{W}, & \mathbf{X}_4 &= s_4 \mathbf{W} & \text{and} & \mathbf{Y}_4 &= \gamma_{L/4}^x s_4 \mathbf{W}. \end{aligned} \quad (11)$$

The coordinates  $(z_1, z_2, z_3, z_4) \in \mathbf{C}^4$  on the center manifold can be introduced as projections in the directions  $\mathbf{X}_j$  and  $\mathbf{Y}_j$ ,  $j = 1, 2, 3, 4$ . The symmetries of the system transform the coordinates in the following way:

$$\begin{aligned} s_1 &: (z_1, z_2, z_3, z_4) \mapsto (z_2, \bar{z}_1, \bar{z}_4, z_3), \\ s_2 &: (z_1, z_2, z_3, z_4) \mapsto (\bar{z}_1, \bar{z}_2, \bar{z}_3, \bar{z}_4), \\ s_3 &: (z_1, z_2, z_3, z_4) \mapsto (\bar{z}_2, z_1, z_4, \bar{z}_3), \\ s_4 &: (z_1, z_2, z_3, z_4) \mapsto (z_1, \bar{z}_2, z_4, z_3), \\ s_5 &: (z_1, z_2, z_3, z_4) \mapsto (\bar{z}_1, z_2, \bar{z}_4, \bar{z}_3), \\ s_6 &: (z_1, z_2, z_3, z_4) \mapsto (z_2, z_1, z_3, \bar{z}_4), \\ s_7 &: (z_1, z_2, z_3, z_4) \mapsto (\bar{z}_2, \bar{z}_1, \bar{z}_3, z_4), \\ \gamma_\alpha^x &: (z_1, z_2, z_3, z_4) \mapsto (e^{2\pi i \alpha / L} z_1, z_2, e^{2\pi i \alpha / L} z_3, e^{2\pi i \alpha / L} z_4), \\ \gamma_\alpha^y &: (z_1, z_2, z_3, z_4) \mapsto (z_1, e^{2\pi i \alpha / L} z_2, e^{2\pi i \alpha / L} z_3, e^{-2\pi i \alpha / L} z_4), \\ r &: (z_1, z_2, z_3, z_4) \mapsto (-z_1, -z_2, -z_3, -z_4). \end{aligned}$$

## 2.2. Normal form

The normal form on center manifold  $\mathbf{C}^4$  for the symmetry group  $\mathbf{D}_4 \times \mathbf{T}^2$  was considered by [18]. In the presence of the Boussinesq symmetry, the even order terms vanish meaning that the normal form with  $\mathbf{D}_4 \times \mathbf{T}^2 \times \mathbf{Z}_2$  symmetry truncated at cubic order is

$$\begin{aligned} \dot{z}_1 &= \lambda_1 z_1 + z_1(A_1 |z_1|^2 + A_2 |z_2|^2 + A_3(|z_3|^2 + |z_4|^2)) + A_4 \bar{z}_1 z_3 \bar{z}_4, \\ \dot{z}_2 &= \lambda_1 z_2 + z_2(A_1 |z_2|^2 + A_2 |z_1|^2 + A_3(|z_3|^2 + |z_4|^2)) + A_4 \bar{z}_2 z_3 \bar{z}_4, \\ \dot{z}_3 &= \lambda_2 z_3 + z_3(A_5 |z_3|^2 + A_6 |z_4|^2 + A_7(|z_1|^2 + |z_2|^2)) + A_8(z_2^2 z_4 + z_1^2 \bar{z}_4), \\ \dot{z}_4 &= \lambda_2 z_4 + z_4(A_5 |z_4|^2 + A_6 |z_3|^2 + A_7(|z_1|^2 + |z_2|^2)) + A_8(\bar{z}_2^2 z_3 + z_1^2 \bar{z}_3), \end{aligned} \quad (12)$$

where  $A_i$  are real numbers (the normal form coefficients). The linear growth rates  $\lambda_1$  and  $\lambda_2$  are close to zero for the truncation to be valid; otherwise higher order terms become important. In Section 4 we relate  $\lambda_i$  and  $A_i$  to the Boussinesq problem for parameters  $(k, R)$  close to  $(k_m, R_m)$  (implying that  $L$  is close to  $L_m$ ).

In polar coordinates  $z_j = r_j e^{i\theta_j}$  (with  $r_j \geq 0$  and  $\theta_j \in [0, 2\pi)$ ) the normal form becomes

$$\begin{aligned} \dot{r}_1 &= r_1(\lambda_1 + A_1 r_1^2 + A_2 r_2^2 + A_3(r_3^2 + r_4^2)) + A_4 r_1 r_3 r_4 \cos(\theta_4 + \theta_3 - 2\theta_1) \\ \dot{r}_2 &= r_2(\lambda_1 + A_1 r_2^2 + A_2 r_1^2 + A_3(r_3^2 + r_4^2)) + A_4 r_2 r_3 r_4 \cos(\theta_3 - 2\theta_2 - \theta_4) \\ \dot{r}_3 &= r_3(\lambda_2 + A_5 r_3^2 + A_6 r_4^2 + A_7(r_1^2 + r_2^2)) + A_8(r_2^2 r_4 \cos(2\theta_2 + \theta_4 - \theta_3) + r_1^2 r_4 \cos(2\theta_1 - \theta_4 - \theta_3)) \\ \dot{r}_4 &= r_4(\lambda_2 + A_5 r_4^2 + A_6 r_3^2 + A_7(r_1^2 + r_2^2)) + A_8(r_2^2 r_3 \cos(\theta_3 - 2\theta_2 - \theta_4) + r_1^2 r_3 \cos(2\theta_1 - \theta_3 - \theta_4)) \\ \dot{\theta}_1 &= A_4 r_3 r_4 \sin(\theta_3 + \theta_4 - 2\theta_1) \\ \dot{\theta}_2 &= A_4 r_3 r_4 \sin(\theta_3 - 2\theta_2 - \theta_4) \\ r_3 \dot{\theta}_3 &= A_8(r_2^2 r_4 \sin(2\theta_2 + \theta_4 - \theta_3) + r_1^2 r_4 \sin(2\theta_1 - \theta_4 - \theta_3)) \\ r_4 \dot{\theta}_4 &= A_8(r_2^2 r_3 \sin(\theta_3 - 2\theta_2 - \theta_4) + r_1^2 r_3 \sin(2\theta_1 - \theta_3 - \theta_4)). \end{aligned} \quad (13)$$

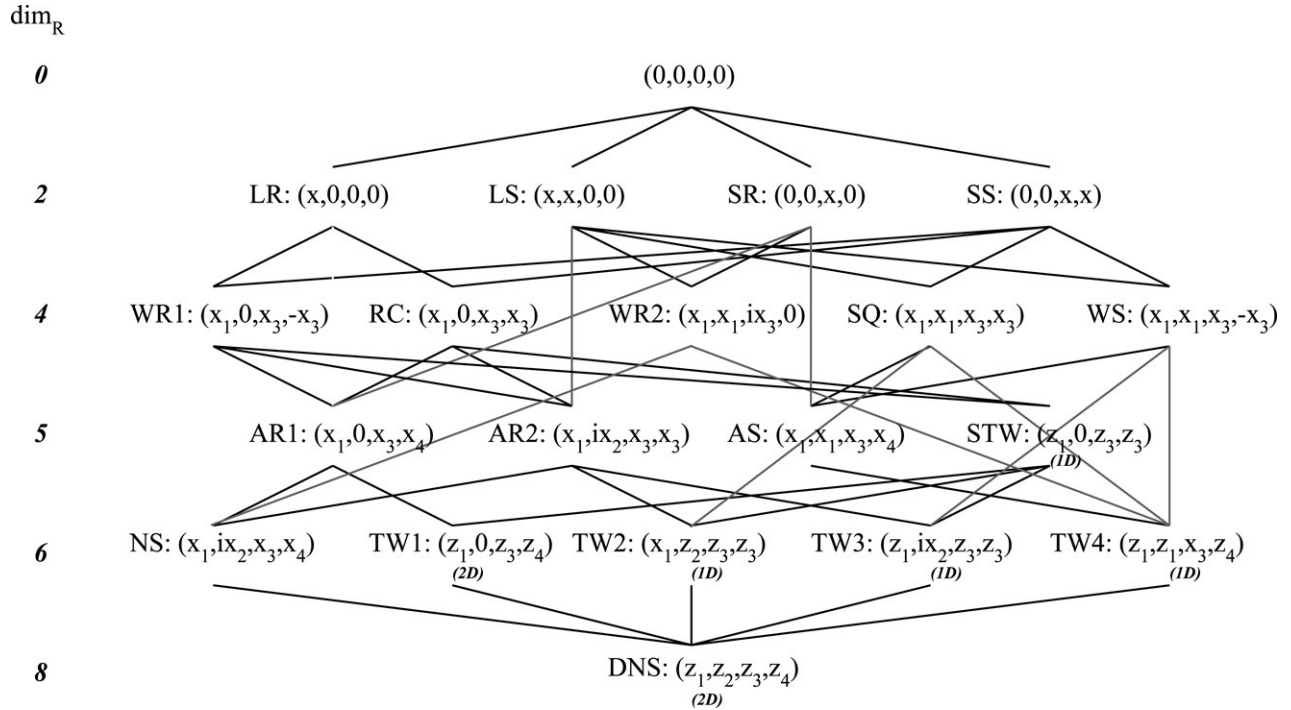


Fig. 2. Lattice of symmetry types of relative equilibria emerging in the normal form (12). The dimensions of the group orbits of these states are shown on the left, and the generic dimension of drift of the drifting states STW, TW1, TW2, TW3, TW4 and DNS (drifting, no symmetry) are shown.

The expressions in the r.h.s. of Eq. (13) involve angles only in the following combinations:  $\phi = 2\theta_1 - \theta_3 - \theta_4$  and  $\psi = 2\theta_2 - \theta_3 + \theta_4$ , and a pattern with constant  $r_j$ ,  $j = 1, 2, 3, 4$ , can be described by the coordinates  $(r_1, r_2, r_3, r_4, \phi, \psi)$ . Note that relative equilibria for Eq. (12) are solutions of Eq. (13) with  $\dot{r}_j = 0$  constant. These drift on the group orbit if either  $\phi \neq 0 \pmod{\pi}$  or  $\psi \neq 0 \pmod{\pi}$ . Below we use the six-dimensional polar coordinates  $(\mathbf{r}, \phi, \psi)$  as well as the four-dimensional complex Cartesian coordinates  $\mathbf{z}$ .

### 3. Bifurcations of the normal form (12) for a general set of coefficients

First we consider the solutions and bifurcation structure for generic choice of the real normal form coefficients  $A_i$ ,  $i = 1, \dots, 8$ . We define the primary bifurcations to be bifurcations of the trivial (non-convecting) state  $(0, 0, 0, 0)$ ; this creates primary branches of solutions. A bifurcation from a primary branch is called a secondary bifurcation and creates secondary branches and similarly a bifurcation from secondary branches is a tertiary bifurcation and creates tertiary branches. The case where a branch starts at a primary branch and ends at a secondary branch is referred to as tertiary. We study bifurcations occurring when  $\lambda_i$  are varied and  $A_j$  are fixed: for convection (see Section 5) this corresponds to a fixed  $P$  and a varying  $R$  and  $L$ . Generic bifurcations of equilibria of different symmetry types occurring in the normal form (12) are summarized in Fig. 2 and the structure of emerging steady states and travelling waves is illustrated in Fig. 3.

For the action of  $\mathbf{D}_4 \times \mathbf{T}^2 \times \mathbf{Z}_2$  on  $\mathbf{C}_4$  that we consider, steady states with symmetry groups not listed in Fig. 2 can exist, for example  $(x_1, x_2, 0, 0)$ ,  $(0, 0, x_3, x_4)$  and  $(x_1, x_2, x_3, x_3)$ , although these are not isolated solutions for the normal form (12). In fact the third-order normal form is degenerate and to resolve the degeneracy some of the fifth-order terms should be included. (See e.g. the study of bifurcations in a  $\mathbf{D}_4$ -symmetric system on  $\mathbf{R}^2$  in [8].) However, these solutions emerge only in the special cases  $A_1 - A_2 = 0$  or  $A_5 - A_6 = 0$ . For the convective system considered in fact these differences are always positive (see Section 4), meaning that the third-order truncation is sufficient.

#### 3.1. Primary bifurcations

Bifurcations from the trivial steady state  $S_0$ ,  $(z_1, z_2, z_3, z_4) = \mathbf{0}$ , take place when  $\lambda_1 = 0$  or  $\lambda_2 = 0$ . In both subspaces the group action is isomorphic to  $\mathbf{D}_4 \times \mathbf{T}^2$ , and therefore branches of steady states listed in Table 1 can be obtained applying standard results.

#### 3.2. Secondary bifurcations

In this subsection we study bifurcations from the primary steady states. To label the bifurcating branches we try to follow the terminology used in [18] as much as possible; however, in our case there are more types of steady state because of the presence of the Boussinesq symmetry.

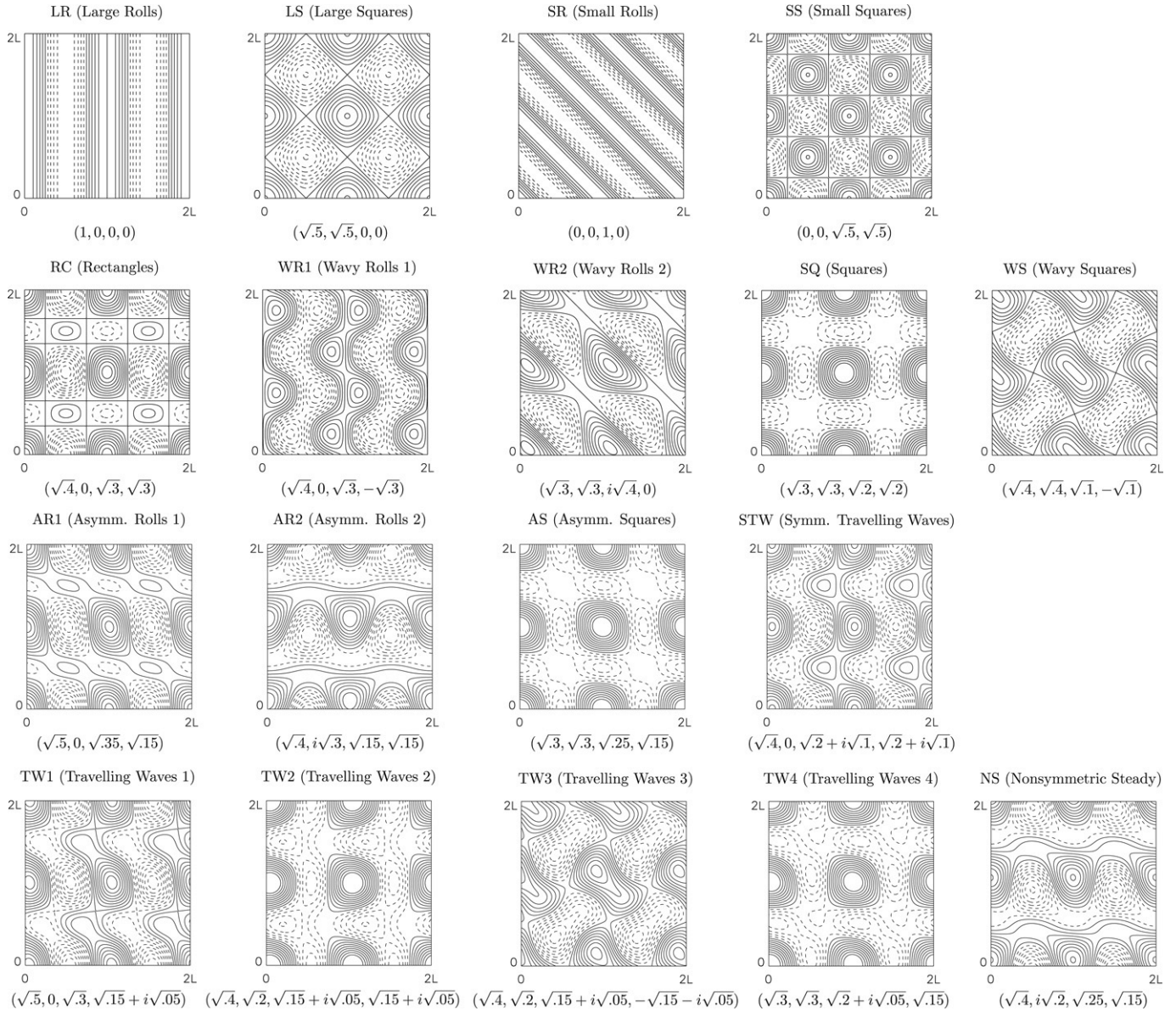


Fig. 3. Isolines (step 0.2) of the vertical component of the velocity in the horizontal mid-plane for convective steady states and travelling waves evaluated for the respective solutions of Eq. (12). Four copies of the periodicity cell are shown for clarity. The relation between convective and solutions of Eq. (12) is given by Eqs. (6), (10) and (11). The numbers below a pattern are coordinates of the pattern on the center manifold in the basis defined by Eq. (11).

Table 1  
Steady state branches bifurcating from  $S_0$ : the condition for occurrence of the bifurcation, label of the bifurcating steady state, the symmetry group of the state, generators of the group, typical point and equation for the branch

Bifurcates at	Name	Group	Generators	Typical point	Amplitude	No
$\lambda_1 = 0$	LR	$\mathbf{D}_2 \times \mathbf{T} \times \mathbf{Z}_2$	$s_2, s_4, \gamma_\alpha^y, \gamma_L^x/2^r$	$(x, 0, 0, 0)$	$x^2 = -\lambda_1/A_1$	1, 29
$\lambda_1 = 0$	LS	$\mathbf{D}_4 \times \mathbf{Z}_2$	$s_1, s_4, \gamma_L^{xy}/2^r$	$(x, x, 0, 0)$	$x^2 = -\lambda_1/(A_1 + A_2)$	1, 29
$\lambda_2 = 0$	SR	$\mathbf{D}_2 \times \mathbf{T} \times \mathbf{Z}_4$	$s_2, s_6, \gamma_\alpha^{x-y}, \gamma_L^{xy}/4^r$	$(0, 0, x, 0)$	$x^2 = -\lambda_2/A_5$	2, 33
$\lambda_2 = 0$	SS	$\mathbf{D}_4 \times \mathbf{Z}_2$	$s_1, s_4, \gamma_L^x/2^r$	$(0, 0, x, x)$	$x^2 = -\lambda_2/(A_5 + A_6)$	2, 33

The last column gives the bifurcation numbers in the order of reference in Sections 4–6.

Table 2 presents eigenspaces and associated eigenvalues of the mapping (12) linearized in the vicinity of the respective steady states. The fifth column gives the action of the steady state symmetry groups on the eigenspaces, and the sixth column indicates which elements of this group act trivially.

Table 2  
Invariant subspaces and associated eigenvalues that determine the stability of respective steady states

Steady state	Typical point	Invariant subspaces	Eigenvalues	Action	Kernel
LR	(x, 0, 0, 0)	(q, 0, 0, 0)	$-2\lambda_1$	<b>1</b>	all
		(iq, 0, 0, 0)	0	<b>Z<sub>2</sub></b>	$s_4, \gamma_\alpha^y, \gamma_{L/2}^x r$
		(0, w, 0, 0)	$\lambda_1(A_1 - A_2)/A_1$	<b>Z<sub>2</sub> × T</b>	$\gamma_{L/2}^{xy} r, s_5$
		(0, 0, w, $\bar{w}$ )	$\lambda_2 + (A_7 + A_8)x^2$	<b>Z<sub>2</sub> × T</b>	$s_5, \gamma_{L/2}^x r$
		(0, 0, w, $-\bar{w}$ )	$\lambda_2 + (A_7 - A_8)x^2$	<b>Z<sub>2</sub> × T</b>	$\gamma_{L/2}^x r, \gamma_{L/2}^y s_5$
LS	(x, x, 0, 0)	(q, q, 0, 0)	$-2\lambda_1$	<b>1</b>	all
		(iq <sub>1</sub> , iq <sub>2</sub> , 0, 0)	0	<b>D<sub>4</sub></b>	$\gamma_{L/2}^{xy} r$
		(q, -q, 0, 0)	$2\lambda_1(A_2 - A_1)/(A_1 + A_2)$	<b>Z<sub>2</sub></b>	$s_2, s_4, \gamma_{L/2}^{xy} r$
		(0, 0, q, q)	$\lambda_2 + 2(A_7 + A_8)x^2$	<b>Z<sub>2</sub></b>	$s_1, s_4$
		(0, 0, q, -q)	$\lambda_2 + 2(A_7 - A_8)x^2$	<b>Z<sub>2</sub></b>	$s_2, \gamma_{L/2}^{xy} r s_1$
		(0, 0, iq <sub>1</sub> , iq <sub>2</sub> )	$\lambda_2 + 2A_7 x^2$	<b>D<sub>4</sub></b>	$\gamma_{L/2}^{xy} r s_2$
SR	(0, 0, x, 0)	(0, 0, q, 0)	$-2\lambda_2$	<b>1</b>	all
		(0, 0, iq, 0)	0	<b>Z<sub>2</sub></b>	$s_6, \gamma_\alpha^{x,-y}, \gamma_{L/4}^{xy} r$
		(0, 0, 0, w)	$\lambda_2(A_5 - A_6)/A_5$	<b>Z<sub>2</sub> × T</b>	$s_7, \gamma_{L/2}^x r$
		(w <sub>1</sub> , w <sub>2</sub> , 0, 0)	$\lambda_1 + A_3 x^2$	<b>D<sub>2</sub> × T × Z<sub>4</sub></b>	
SS	(0, 0, x, x)	(0, 0, q, q)	$-2\lambda_2$	<b>1</b>	all
		(0, 0, iq <sub>1</sub> , iq <sub>2</sub> )	0	<b>D<sub>4</sub></b>	$\gamma_{L/2}^x r$
		(0, 0, q, -q)	$2\lambda_2(A_6 - A_5)/(A_5 + A_6)$	<b>Z<sub>2</sub></b>	$s_2, s_6, \gamma_{L/2}^x r$
		(q <sub>1</sub> , q <sub>2</sub> , 0, 0)	$\lambda_1 + (2A_3 + A_4)x^2$	<b>D<sub>4</sub></b>	$s_2, s_4$
		(iq <sub>1</sub> , iq <sub>2</sub> , 0, 0)	$\lambda_1 + (2A_3 - A_4)x^2$	<b>D<sub>4</sub></b>	$s_4 \gamma_{L/2}^x r, s_5 \gamma_{L/2}^y r$

The fifth column gives the action of the steady state symmetry groups on the subspace and the sixth column gives the generators of the kernel of this action.

Table 3  
Branches of steady states bifurcating from LR, LS, SR and SS

Bifurcates at	Name	Group	Generators	Typical point	No
FROM LR = (x, 0, 0, 0)					
$\lambda_2 + (A_7 + A_8)x^2 = 0$	RC	<b>D<sub>2</sub> × Z<sub>2</sub></b>	$s_2, s_5, \gamma_{L/2}^x r$	(x <sub>1</sub> , 0, x <sub>3</sub> , x <sub>3</sub> )	17
$\lambda_2 + (A_7 - A_8)x^2 = 0$	WR1	<b>D<sub>2</sub> × Z<sub>2</sub></b>	$s_2, \gamma_{L/2}^y s_5, \gamma_{L/2}^x r$	(x <sub>1</sub> , 0, x <sub>3</sub> , -x <sub>3</sub> )	25
FROM LS = (x, x, 0, 0)					
$\lambda_2 = -2(A_7 + A_8)x^2$	SQ	<b>D<sub>4</sub></b>	$s_1, s_4$	(x <sub>1</sub> , x <sub>1</sub> , x <sub>3</sub> , x <sub>3</sub> )	12
$\lambda_2 = -2(A_7 - A_8)x^2$	WS	<b>D<sub>4</sub></b>	$\gamma_{L/2}^{xy} r s_1, s_6$	(x <sub>1</sub> , x <sub>1</sub> , x <sub>3</sub> , -x <sub>3</sub> )	24
$\lambda_2 + 2A_7 x^2 = 0$	AR2	<b>D<sub>2</sub></b>	$s_4, \gamma_{L/2}^{xy} r s_2$	(x <sub>1</sub> , x <sub>2</sub> , ix <sub>3</sub> , ix <sub>3</sub> )	18
$\lambda_2 + 2A_7 x^2 = 0$	WR2	<b>D<sub>2</sub></b>	$s_6, \gamma_{L/2}^{xy} r s_2$	(x <sub>1</sub> , x <sub>1</sub> , ix <sub>3</sub> , 0)	18
FROM SR = (0, 0, x, 0)					
$\lambda_1 + A_3 x^2 = 0$	WR2	<b>D<sub>2</sub></b>	$\gamma_{L/2}^y r s_2, \gamma_{L/4}^{x,-y} s_6$	(ix <sub>1</sub> , x <sub>1</sub> , x <sub>3</sub> , 0)	26
$\lambda_1 + A_3 x^2 = 0$	AR1	<b>D<sub>2</sub></b>	$s_2, \gamma_{L/2}^y r$	(x <sub>1</sub> , 0, x <sub>3</sub> , x <sub>4</sub> )	26
$\lambda_1 + A_3 x^2 = 0$	AS	<b>D<sub>2</sub></b>	$s_2, s_6$	(x <sub>1</sub> , x <sub>1</sub> , x <sub>3</sub> , x <sub>4</sub> )	26
FROM SS = (0, 0, x, x)					
$\lambda_1 + (2A_3 + A_4)x^2 = 0$	SQ	<b>D<sub>4</sub></b>	$s_1, s_4$	(x <sub>1</sub> , x <sub>1</sub> , x <sub>3</sub> , x <sub>3</sub> )	3
$\lambda_1 + (2A_3 + A_4)x^2 = 0$	RC	<b>D<sub>2</sub> × Z<sub>2</sub></b>	$s_2, s_5, \gamma_{L/2}^x r$	(x <sub>1</sub> , 0, x <sub>3</sub> , x <sub>3</sub> )	3
$\lambda_1 + (2A_3 - A_4)x^2 = 0$	WS	<b>D<sub>4</sub></b>	$\gamma_{L/2}^x r s_1, s_6$	(ix <sub>1</sub> , ix <sub>1</sub> , x <sub>3</sub> , x <sub>3</sub> )	32
$\lambda_1 + (2A_3 - A_4)x^2 = 0$	WR1	<b>D<sub>2</sub> × Z<sub>2</sub></b>	$s_4, \gamma_{L/2}^{xy} s_2, \gamma_{L/2}^x r$	(ix <sub>1</sub> , 0, x <sub>3</sub> , x <sub>3</sub> )	32

Columns are the same as in Table 1.

Bifurcation takes places if an eigenvalue crosses the imaginary axis. From the action of the symmetry group on the associated eigenspace we determine branches of bifurcating solutions, using results [8] for the respective group. Bifurcations from primary branches are listed in Table 3. Branching equations can be obtained by substitution of expressions for steady states into Eq. (12); they are cumbersome and not listed here. We did not find in the literature any analysis of bifurcations with the symmetry group **D<sub>2</sub> × T × Z<sub>4</sub>** (from SR); hence we include branching and the stability conditions for the branches for this group as Appendix A.

### 3.3. Tertiary bifurcations

In this subsection we consider stability and bifurcation of secondary steady states, i.e. those connecting branches of primary steady states. They have symmetry groups isomorphic to **D<sub>4</sub>**, **D<sub>2</sub> × Z<sub>2</sub>** or to **D<sub>2</sub>**. Similarly to above, to determine stability we

Table 4  
Invariant subspaces and associated eigenvalues determining stability of secondary steady states

Steady state	Typical point	Invariant subspaces	Eigenvalues	Action	Kernel
RC	$(x_1, 0, x_3, x_3)$	$(q_1, 0, q_3, q_3)$	$\mu_1 + \mu_2 = 2A_1x_1^2 + 2(A_5 + A_6)x_3^2$ $\mu_1\mu_2 = 4x_1^2x_3^2(A_1(A_5 + A_6) - (2A_3 + A_4)(A_7 + A_8))$	<b>1</b>	all
		$(0, q, 0, 0)$	$(A_2 - A_1)x_1^2$	<b>Z<sub>2</sub></b>	$s_2, s_5$
		$(0, iq, 0, 0)$	$(A_2 - A_1)x_1^2 - 2A_4x_3^2$	<b>Z<sub>2</sub></b>	$s_5, \gamma_{L/2}^x r s_2$
		$(0, 0, q, -q)$	$2(A_5 - A_6)x_3^2 - 2A_8x_1^2$	<b>Z<sub>2</sub></b>	$s_2, \gamma_{L/2}^x r$
		$(0, 0, iq, -iq)$	0	<b>Z<sub>2</sub></b>	$s_5, \gamma_{L/2}^x r$
		$(iq_1, 0, iq_3, iq_3)$	$0, -2A_8x_1^2 - 2A_4x_3^2$	<b>Z<sub>2</sub></b>	$s_4, \gamma_{L/2}^x r$
WR1	$(x_1, 0, x_3, -x_3)$	$(q_1, 0, q_3, -q_3)$	$\mu_1 + \mu_2 = 2A_1x_1^2 + 2(A_5 + A_6)x_3^2$ $\mu_1\mu_2 = 4x_1^2x_3^2(A_1(A_5 + A_6) - (2A_3 - A_4)(A_7 - A_8))$	<b>1</b>	all
		$(0, q, 0, 0)$	$(A_2 - A_1)x_1^2$	<b>Z<sub>2</sub></b>	$s_2, \gamma_{L/2}^{xy} r s_5$
		$(0, iq, 0, 0)$	$(A_2 - A_1)x_1^2 + 2A_4x_3^2$	<b>Z<sub>2</sub></b>	$\gamma_{L/2}^x r s_2, \gamma_{L/2}^{xy} r s_5$
		$(0, 0, q, q)$	$2(A_5 - A_6)x_3^2 + 2A_8x_1^2$	<b>Z<sub>2</sub></b>	$s_2, \gamma_{L/2}^x r$
		$(0, 0, iq, iq)$	0	<b>Z<sub>2</sub></b>	$\gamma_{L/2}^x r, \gamma_{L/2}^y s_5$
		$(iq_1, 0, iq_3, -iq_3)$	$0, 2A_8x_1^2 + 2A_4x_3^2$	<b>Z<sub>2</sub></b>	$\gamma_{L/2}^x r, \gamma_{L/2}^y s_4$
WR2	$(x_1, x_1, ix_3, 0)$	$(q_1, q_1, iq_3, 0)$	$\mu_1 + \mu_2 = 2(A_1 + A_2)x_1^2 + 2A_5x_3^2$ $\mu_1\mu_2 = 4x_1^2x_3^2((A_1 + A_2)A_5 - 2A_3A_7)$	<b>1</b>	all
		$(q_1, -q_1, 0, iq_4)$	$\mu_1 + \mu_2 = 2(A_1 - A_2)x_1^2 + (A_6 - A_5)x_3^2$ $\mu_1\mu_2 = 4x_1^2x_3^2((A_1 - A_2)(A_6 - A_5) - A_3A_8)$	<b>Z<sub>2</sub></b>	$\gamma_{L/2}^{xy} r s_2$
		$(iq_1, -iq_1, 0, 0)$	0	<b>Z<sub>2</sub></b>	$\gamma_{L/2}^{xy} r s_7$
		$(iq_1, iq_1, q_3, q_4)$	$\mu_1 = 0$ $\mu_2 + \mu_3 = (A_6 - A_5)x_3^2$ $\mu_2\mu_3 = -4A_8x_1^2(A_8x_1^2 + A_4x_3^2)$	<b>Z<sub>2</sub></b>	$s_6$
SQ	$(x_1, x_1, x_3, x_3)$	$(q_1, q_1, q_3, q_3)$	$\mu_1 + \mu_2 = 2(A_1 + A_2)x_1^2 + 2(A_5 + A_6)x_3^2$ $\mu_1\mu_2 = 4x_1^2x_3^2((A_1 + A_2)(A_5 + A_6) - 2(2A_3 + A_4)(A_7 + A_8))$	<b>1</b>	all
		$(q, -q, 0, 0)$	$2(A_1 - A_2)x_1^2$	<b>Z<sub>2</sub></b>	$s_2, s_4$
		$(0, 0, q, -q)$	$2(A_5 - A_6)x_3^2 - 4A_8x_1^2$	<b>Z<sub>2</sub></b>	$s_2, s_6$
		$(iq_1, iq_2, iq_3, iq_4)$	$\mu_1 = \mu_2 = 0$ $\mu_3 = \mu_4 = -2A_8x_1^2 - 2A_4x_3^2$	<b>D<sub>4</sub></b>	
WS	$(x_1, x_1, x_3, -x_3)$	$(q_1, q_1, q_3, -q_3)$	$\mu_1 + \mu_2 = 2(A_1 + A_2)x_1^2 + 2(A_5 + A_6)x_3^2$ $\mu_1\mu_2 = 4x_1^2x_3^2((A_1 + A_2)(A_5 + A_6) - 2(2A_3 - A_4)(A_7 - A_8))$	<b>1</b>	all
		$(q, -q, 0, 0)$	$2(A_1 - A_2)x_1^2$	<b>Z<sub>2</sub></b>	$s_2, \gamma_{L/2}^{xy} r s_5$
		$(0, 0, q, q)$	$2(A_5 - A_6)x_3^2 + 4A_8x_1^2$	<b>Z<sub>2</sub></b>	$s_2, s_6$
		$(iq_1, iq_2, iq_3, iq_4)$	$\mu_1 = \mu_2 = 0$ $\mu_3 = \mu_4 = 2A_8x_1^2 + 2A_4x_3^2$	<b>D<sub>4</sub></b>	

Columns are the same as in Table 2.

decompose  $\mathbf{C}^4$  into isotypic components for the action of the groups and calculate the eigenvalues of the linearization of Eq. (12) near the steady state, restricted to the respective subspace. The results of calculations are presented in the Table 4.

Bifurcations from secondary branches (see Table 5) are investigated in the same way those from primary branches. Some of these bifurcations give rise to branches of drifting patterns (we refer to as travelling waves). Examples of such bifurcations are discussed in Appendix B.

### 3.4. Bifurcations from tertiary branches

Here we focus on bifurcations from AR1, AR2, AS and STW which all have symmetry groups isomorphic to  $\mathbf{D}_2$ . Methods and presentation are the same as above for more symmetric steady states. We do not list expressions for eigenvalues in the cases where isotypic components are three-dimensional because they are unwieldy and uninformative. In Appendix C we give an example how bifurcations in a three-dimensional subspace can be studied without explicitly evaluating the eigenvalues. Tertiary branches and eigenvalues determining their stability are listed in Table 6, and possible bifurcations in Table 7.

### 3.5. Robust heteroclinic connections between steady states

A heteroclinic connection from one steady state to another one is robust only if there exists such a fixed point subspace for a subgroup of the system symmetry group such that the connection within that subspace is robust [12], for example if it is a saddle

Table 5  
Bifurcations from secondary steady states

Bifurcates at	Name	Group	Generators	Typical point	No
FROM RC = $(x_1, 0, x_3, x_3)$ $2A_1x_1^2 + 2(A_5 + A_6)x_3^2 = 0$ $(A_2 - A_1)x_1^2 - 2A_4x_3^2 = 0$ $(A_5 - A_6)x_3^2 = A_8x_1^2$ $A_8x_1^2 = -A_4x_3^2$	P(RC) AR2 AR1 STW	$\mathbf{D}_2 \times \mathbf{Z}_2$ $\mathbf{D}_2$ $\mathbf{D}_2$ $\mathbf{D}_2$	$s_2, s_5, \gamma_{L/2}^x r$ $s_5, \gamma_{L/2}^x r s_2$ $s_2, \gamma_{L/2}^x r$ $s_4, \gamma_{L/2}^x r$	$(x_1, 0, x_3, x_3)$ (periodic orbit) $(x_1, ix_2, x_3, x_3)$ $(x_1, 0, x_3, x_4)$ $(z_1, 0, z_3, z_3) = (r_1, 0, r_3, r_3, \phi, 0)$	13 5 8
FROM WR1 = $(x_1, 0, x_3, -x_3)$ $2A_1x_1^2 + 2(A_5 + A_6)x_3^2 = 0$ $(A_2 - A_1)x_1^2 + 2A_4x_3^2 = 0$ $(A_5 - A_6)x_3^2 + A_8x_1^2 = 0$ $A_8x_1^2 + A_4x_3^2 = 0$	P(WR1) AR2 AR1 STW	$\mathbf{D}_2 \times \mathbf{Z}_2$ $\mathbf{D}_2$ $\mathbf{D}_2$ $\mathbf{D}_2$	$s_2, \gamma_{L/2}^y s_5, \gamma_{L/2}^x r$ $\gamma_{L/2}^y s_4, \gamma_{L/2}^x r s_2$ $s_2, \gamma_{L/2}^x r$ $\gamma_{L/2}^y s_4, \gamma_{L/2}^x r$	$(x_1, 0, x_3, -x_3)$ (periodic orbit) $(x_1, ix_2, x_3, -x_3)$ $(x_1, 0, x_3, x_4)$ $(z_1, 0, z_3, -z_3) = (r_1, 0, r_3, r_3, \phi, \pi)$	31
FROM WR2 = $(x_1, x_1, ix_3, 0)$ $(A_1 + A_2)x_1^2 + 2A_5x_3^2 = 0$ $(A_1 - A_2)(A_6 - A_5) - A_3A_8 = 0$ $2(A_1 - A_2)x_1^2 + (A_6 - A_5)x_3^2 = 0$ $A_8x_1^2 + A_4x_3^2 = 0$	P(WR2) NS P(NS) TW4	$\mathbf{D}_2$ $\mathbf{Z}_2$ $\mathbf{Z}_2$ $\mathbf{Z}_2$	$s_6, \gamma_{L/2}^{xy} r s_2$ $\gamma_{L/2}^{xy} r s_2$ $\gamma_{L/2}^{xy} r s_2$ $s_6$	$(x_1, x_1, ix_3, 0)$ (periodic orbit) $(x_1, x_2, ix_3, ix_4)$ $(x_1, x_2, ix_3, ix_4)$ (periodic orbit) $(z_1, z_1, z_3, x_4) = (r_1, r_1, r_3, r_4, \phi, -\phi)$	20 19
FROM SQ = $(x_1, x_1, x_3, x_3)$ $(A_1 + A_2)x_1^2 + (A_5 + A_6)x_3^2 = 0$ $(A_5 - A_6)x_3^2 - 2A_8x_1^2 = 0$ $A_8x_1^2 + A_4x_3^2 = 0$ $A_8x_1^2 + A_4x_3^2 = 0$	P(SQ) AS TW2 TW4	$\mathbf{D}_4$ $\mathbf{D}_2$ $\mathbf{Z}_2$ $\mathbf{Z}_2$	$s_1, s_4$ $s_2, s_6$ $s_4$ $s_6$	$(x_1, x_1, x_3, x_3)$ (periodic orbit) $(x_1, x_1, x_3, x_4)$ $(z_1, x_2, z_3, z_3) = (r_1, r_2, r_3, r_3, \phi, 0)$ $(z_1, z_1, z_3, z_4) = (r_1, r_1, r_3, r_4, \phi, \phi)$	4 9 9
FROM WS = $(x_1, x_1, x_3, -x_3)$ $(A_1 + A_2)x_1^2 + (A_5 + A_6)x_3^2 = 0$ $(A_5 - A_6)x_3^2 + 2A_8x_1^2 = 0$ $A_8x_1^2 + A_4x_3^2 = 0$ $A_8x_1^2 + A_4x_3^2 = 0$	P(WS) AS TW3 TW4	$\mathbf{D}_4$ $\mathbf{D}_2$ $\mathbf{Z}_2$ $\mathbf{Z}_2$	$\gamma_{L/2}^{xy} r s_1, s_6$ $s_2, s_6$ $\gamma_{L/2}^{xy} r s_4$ $s_6$	$(x_1, x_1, x_3, -x_3)$ (periodic orbit) $(x_1, x_1, x_3, x_4)$ $(z_1, x_2, z_3, -z_3) = (r_1, r_2, r_3, r_3, \phi, \pi)$ $(z_1, z_1, z_3, z_4) = (r_1, r_1, r_3, r_4, \phi, -\phi)$	27 27

Columns are the same as in Table 1.  $P(M)$  indicates there is bifurcation to periodic orbits with instantaneous symmetry equal to that of  $M$ .

Table 6  
Invariant subspaces and associated eigenvalues determining stability of tertiary branches of relative equilibria

Steady state	Typical point	Invariant subspaces	Eigenvalues	Action	Kernel
AR1	$(x_1, 0, x_3, x_4)$	$(q_1, 0, q_3, q_4)$ $(iq_1, 0, iq_3, iq_4)$ $(0, q, 0, 0)$ $(0, iq, 0, 0)$	$\mu_1, \mu_2, \mu_3$ $0, 0, -A_8x_1^2(x_4/x_3 + x_3/x_4) - 2A_4x_3x_4$ $(A_2 - A_1)x_1^2$ $(A_2 - A_1)x_1^2 - 2A_4x_3x_4$	$\mathbf{1}$ $\mathbf{Z}_2$ $\mathbf{Z}_2$ $\mathbf{Z}_2$	All $\gamma_{L/2}^x r$ $s_2$ $\gamma_{L/2}^x r s_2$
AR2	$(x_1, ix_2, x_3, x_3)$	$(q_1, iq_2, q_3, q_3)$ $(iq_1, 0, iq_3, iq_3)$ $(0, q_2, iq_3, -iq_3)$ $(0, 0, q, -q)$	$\mu_1, \mu_2, \mu_3$ $0, -2A_8x_1^2 - 2A_4x_3^2$ $0, 2A_8x_2^2 + 2A_4x_3^2$ $2A_8(-x_1^2 + x_2^2) + 2(A_5 - A_6)x_3^2$	$\mathbf{1}$ $\mathbf{Z}_2$ $\mathbf{Z}_2$ $\mathbf{Z}_2$	All $\gamma_{L/2}^x s_4$ $s_5$ $\gamma_{L/2}^x s_2$
AS	$(x_1, x_1, x_3, x_4)$	$(q_1, q_1, q_3, q_4)$ $(iq_1, iq_1, iq_3, 0)$ $(iq_1, -iq_1, 0, iq_4)$ $(q, -q, 0, 0)$	$\mu_1, \mu_2, \mu_3$ $0, -2A_8x_1^2x_4/x_3 - 2A_4x_3x_4$ $0, -2A_8x_1^2x_3/x_4 - 2A_4x_3x_4$ $2(A_1 - A_2)x_1^2$	$\mathbf{1}$ $\mathbf{Z}_2$ $\mathbf{Z}_2$ $\mathbf{Z}_2$	All $s_6$ $s_7$ $s_2$
STW	$(z_1, 0, z_3, z_3) =$ $(r_1, 0, r_3, r_3, \phi, 0)$	$(q_1, 0, q_2, q_2, \xi, 0)$ $(0, q, 0, 0)$ $(0, iq, 0, 0)$ $(0, 0, w, -w)$	$\mu_1, \mu_2, \mu_3$ $(A_2 - A_1)r_1^2 + A_4r_3^2(1 - \cos \phi)$ $(A_2 - A_1)r_1^2 - A_4r_3^2(1 + \cos \phi)$ $0, 2(A_5 - A_6)r_3^2 - 2A_8r_1^2 \cos \phi$	$\mathbf{1}$ $\mathbf{Z}_2$ $\mathbf{Z}_2$ $\mathbf{Z}_2$	All $s_4$ $\gamma_{L/2}^x r s_4$ $\gamma_{L/2}^x r$

Note that AR1, AR2, AS are steady solutions whereas STW are drifting (travelling waves). Columns are the same as in Table 2.

to sink connection. Examination of Table 2 reveals the possibility of robust heteroclinic connections given in Table 8 where we list pairs of steady states between which robust heteroclinic connections are possible.

The connections within subspaces listed in Table 8 can form homoclinic and heteroclinic cycles, e.g. the connection  $SS \rightarrow SS$  implies existence of the respective homoclinic cycle. There are three subspaces in which connections between LS and SS are

Table 7  
Bifurcations from tertiary branches

Bifurcates at	Name	Group	Generators	Typical point	No
FROM AR1 = $(x_1, 0, x_3, x_4)$ $\mu_1 = i\omega, \mu_2 = -i\omega$	P(AR1)	$\mathbf{D}_2$	$s_2, \gamma_{L/2}^x r$	$(x_1, 0, x_3, x_4)$ (periodic orbit)	7
$A_8 x_1^2 (x_4/x_3 + x_3/x_4) + A_4 x_3 x_4 = 0$	TW1	$\mathbf{Z}_2$	$\gamma_{L/2}^x r$	$(z_1, 0, z_3, z_4) = (r_1, 0, r_3, r_4, \phi, \psi)$	11
$(A_2 - A_1)x_1^2 - 2A_4 x_3 x_4 = 0$	NS	$\mathbf{Z}_2$	$\gamma_{L/2}^x r s_2$	$(x_1, ix_2, x_3, x_4)$	
FROM AR2 = $(x_1, ix_2, x_3, x_3)$ $\mu_1 = i\omega, \mu_2 = -i\omega$	P(AR2)	$\mathbf{D}_2$	$s_5, \gamma_{L/2}^y r s_2$	$(x_1, ix_2, x_3, x_3)$ (periodic orbit)	
$A_8 x_1^2 + A_4 x_3^2 = 0$	TW3	$\mathbf{Z}_2$	$\gamma_{L/2}^y r s_4$	$(z_1, ix_2, z_3, z_3) = (r_1, r_2, r_3, r_3, \phi, \pi)$	
$A_8 x_2^2 + A_4 x_3^2 = 0$	TW2	$\mathbf{Z}_2$	$s_5$	$(x_1, z_2, z_3, \bar{z}_3) = (r_1, r_2, r_3, r_3, 0, \phi)$	14
$A_8(-x_1^2 + x_2^2) + (A_5 - A_6)x_3^2 = 0$	NS	$\mathbf{Z}_2$	$\gamma_{L/2}^y r s_2$	$(x_1, ix_2, x_3, x_4)$	
FROM AS = $(x_1, x_1, x_3, x_4)$ $\mu_1 = i\omega, \mu_2 = -i\omega$	P(AS)	$\mathbf{D}_2$	$s_2, s_6$	$(x_1, x_1, x_3, x_4)$ (periodic orbit)	6
$A_8 x_1^2 x_4/x_3 + A_4 x_3 x_4 = 0$	TW4	$\mathbf{Z}_2$	$s_6$	$(z_1, z_1, z_3, x_4) = (r_1, r_1, r_3, r_4, \phi, \phi)$	
$A_8 x_1^2 x_3/x_4 + A_4 x_3 x_4 = 0$	TW4	$\mathbf{Z}_2$	$s_7$	$(z_1, \bar{z}_1, x_3, z_4) = (r_1, r_1, r_3, r_4, \phi, -\phi)$	10
FROM STW = $(r_1, 0, r_3, r_3, \phi, 0)$ $\mu_1 = i\omega, \mu_2 = -i\omega$	P(STW)	$\mathbf{D}_2$	$s_4, \gamma_{L/2}^x r$	$(z_1, 0, z_3, z_3)$ (periodic orbit)	28
$(A_2 - A_1)r_1^2 + A_4 r_3^2(1 - \cos \phi) = 0$	TW2	$\mathbf{Z}_2$	$s_4$	$(z_1, x_2, z_3, z_3) = (r_1, r_2, r_3, r_3, \phi, 0)$	
$(A_2 - A_1)r_1^2 - A_4 r_3^2(1 + \cos \phi) = 0$	TW3	$\mathbf{Z}_2$	$\gamma_{L/2}^x r s_4$	$(z_1, ix_2, z_3, z_3) = (r_1, r_2, r_3, r_3, \phi, \pi)$	30
$2(A_5 - A_6)r_3^2 - 2A_8 r_1^2 \cos \phi = 0$	TW1	$\mathbf{Z}_2$	$\gamma_{L/2}^x r$	$(z_1, 0, z_3, z_4) = (r_1, 0, r_3, r_4, \phi, \psi)$	21

Columns are the same as in Table 1.

possible. If there exists a connection  $LS \rightarrow SS$  in one of them, and  $SS \rightarrow LS$  in another one, a heteroclinic cycle  $LS \rightarrow SS \rightarrow LS$  emerges. The system can possess other types of heteroclinic cycles, for example  $LR \rightarrow SS \rightarrow LR$  and  $LS \rightarrow SS \rightarrow SR \rightarrow LS$ , and much more intricate heteroclinic networks.

The two-dimensional subspaces listed in Table 8 are of special interest because for them it is possible to derive analytically a sufficient condition for existence of a heteroclinic connection. Existence of the connection if one state of a pair is stable and another one is unstable is implied by the following theorem that is a modification of Theorem 1 from [9].

**Theorem 1.** Consider the system

$$\begin{aligned}\dot{x} &= \lambda x + B_1 x^3 + B_2 x y^2, \\ \dot{y} &= \mu y + C_1 y^3 + C_2 x^2 y.\end{aligned}$$

If  $\lambda > 0, \mu > 0, B_1 < 0, C_1 < 0, \lambda - B_2 \mu / C_1 > 0, \mu - C_2 \lambda / B_1 < 0$ , then the only steady states of the system are  $(0, 0), S_1 = (\pm \sqrt{-\lambda / B_1}, 0), S_2 = (0, \pm \sqrt{-\mu / C_1})$  and there exists a robust heteroclinic connection from  $S_1$  to  $S_2$ .

#### 4. Analysis of bifurcations of the reduced system

Consider the original motivating hydrodynamic problem of Boussinesq convection in a layer, equations (1)–(4), for parameters  $k$  and  $R$  close to the mode interaction point  $(k_m, R_m)$  shown in Fig. 1. We set

$$\epsilon = R - R_m, \quad \delta = k - k_m, \quad (14)$$

and assume  $\epsilon$  and  $\delta$  are small, so that a center manifold approximation performed in the vicinity of  $(k_m, R_m)$  is valid. Details of calculation of the normal form Eq. (12) coefficients are given in Appendices D–F. The coefficients have dependence on  $P$  given by

$$\lambda_i = P(P+1)^{-1}(\beta_{i1}\delta + \beta_{i2}\epsilon) + O(\epsilon^2 + \delta^2) \quad (15)$$

$$A_i = P(P+1)^{-1}(P^{-2}\alpha_{i1} + P^{-1}\alpha_{i2} + \alpha_{i3}) + O(|\epsilon| + |\delta|). \quad (16)$$

The values of  $\alpha_{ij}$  and  $\beta_{ij}$  are listed in Table 9. The  $\alpha$ 's agree with those in [18]: if the variables in Eq. (12) are rescaled  $z_i \rightarrow \gamma_i z_i$  with  $\gamma_1 = \gamma_2 = \sqrt{A_1^{PM}/A_1}$  and  $\gamma_3 = \gamma_4 = \sqrt{A_5^{PM}/A_5}$ , where the superscript  $PM$  denotes the respective coefficients in the paper [18], the values of the  $\alpha$ 's differ only in the last shown digit.

##### 4.1. A summary of bifurcations for the reduced system for fixed $P$

We investigate the dynamics of the Boussinesq problem near  $(k_m, R_m)$  shown in Fig. 1 for a range of Prandtl numbers  $P$ . We use numerical path following [7] and the results from Section 3.

Table 8

Fixed points subspaces for subgroups of  $\mathbf{D}_4 \times \mathbf{T}^2 \times \mathbf{Z}_2$ , in which robust heteroclinic connections are possible

Subspace	Subgroup	Generators	Steady states	Eigenspaces	Eigenvalues
$(q_1, q_2, iq_3, iq_3)$	$\mathbf{D}_2$	$s_4, \gamma_{L/2}^{xy} r s_2$	LR = $(x, 0, 0, 0)$	$(q, 0, 0, 0)$ $(0, q, 0, 0)$ $(0, 0, iq, iq)$	$-2\lambda_1$ $\lambda_1(A_1 - A_2)/A_1$ $\lambda_2 + (A_7 - A_8)x_1^2$
			LR = $(0, x, 0, 0)$	$(0, q, 0, 0)$ $(q, 0, 0, 0)$ $(0, 0, iq, iq)$	$-2\lambda_1$ $\lambda_1(A_1 - A_2)/A_1$ $\lambda_2 + (A_7 + A_8)x_1^2$
$(q_1, q_2, 0, 0)$	$\mathbf{D}_2 \times \mathbf{Z}_2$	$s_2, s_4, \gamma_{L/2}^{xy} r$	LR = $(x_1, 0, 0, 0)$	$(q, 0, 0, 0)$ $(0, q, 0, 0)$	$-2\lambda_1$ $\lambda_1(A_1 - A_2)/A_1$
			LS = $(x_2, x_2, 0, 0)$	$(q, q, 0, 0)$ $(q, -q, 0, 0)$	$-2\lambda_1$ $\lambda_1(A_2 - A_1)/(A_1 + A_2)$
$(0, 0, q_1, q_2)$	$\mathbf{D}_2 \times \mathbf{Z}_2$	$s_2, s_6, \gamma_{L/2}^{xy}$	SR = $(0, 0, x_1, 0)$	$(0, 0, q, 0)$ $(0, 0, 0, q)$	$-2\lambda_2$ $\lambda_2(A_5 - A_6)/A_5$
			SS = $(0, 0, x_2, x_2)$	$(0, 0, q, q)$ $(0, 0, q, -q)$	$-2\lambda_2$ $\lambda_2(A_6 - A_5)/(A_6 + A_5)$
$(q_1, 0, q_2, q_3)$	$\mathbf{D}_2$	$s_2, \gamma_{L/2}^x r$	SS = $(0, 0, x, x)$	$(0, 0, q, q)$ $(0, 0, q, -q)$	$-2\lambda_2$ $\lambda_2(A_6 - A_5)/(A_6 + A_5)$
			SS = $(0, 0, -x, x)$	$(q, 0, 0, 0)$ $(0, 0, -q, q)$	$\lambda_1 + (2A_3 + A_4)x^2$ $-2\lambda_2$
$(q_1, 0, q_2, q_3)$	$\mathbf{D}_2$	$s_2, \gamma_{L/2}^x r$	LR = $(x_1, 0, 0, 0)$	$(q, 0, 0, 0)$ $(0, 0, q, q)$	$-2\lambda_1$ $\lambda_2 + (A_7 + A_8)x_1^2$
			SR = $(0, 0, x_2, 0)$	$(0, 0, q, -q)$ $(0, 0, q, 0)$ $(0, 0, 0, q)$	$\lambda_2 + (A_7 - A_8)x_1^2$ $-2\lambda_2$ $\lambda_2(A_5 - A_6)/A_5$
$(q_1, 0, q_2, q_2)$	$\mathbf{D}_2 \times \mathbf{Z}_2$	$s_2, s_4, \gamma_{L/2}^x r$	LR = $(x_1, 0, 0, 0)$	$(q, 0, 0, 0)$ $(0, 0, q, q)$	$-2\lambda_1$ $\lambda_2 + (A_7 + A_8)x_1^2$
			SS = $(0, 0, x_2, x_2)$	$(0, 0, q, q)$ $(q, 0, 0, 0)$	$-2\lambda_2$ $\lambda_1 + (2A_3 + A_4)x_2^2$
$(q_1, 0, q_2, -q_2)$	$\mathbf{D}_2 \times \mathbf{Z}_2$	$s_2, \gamma_{L/2}^y s_4, \gamma_{L/2}^x r$	LR = $(x_1, 0, 0, 0)$	$(q, 0, 0, 0)$ $(0, 0, q, -q)$	$-2\lambda_1$ $\lambda_2 + (A_7 - A_8)x_1^2$
			SS = $(0, 0, x_2, -x_2)$	$(0, 0, q, -q)$ $(q, 0, 0, 0)$	$-2\lambda_2$ $\lambda_1 + (2A_3 - A_4)x_2^2$
$(q_1, q_1, q_2, q_2)$	$\mathbf{D}_4$	$s_1, s_4$	LS = $(x_1, x_1, 0, 0)$	$(q, q, 0, 0)$ $(0, 0, q, q)$	$-2\lambda_1$ $\lambda_2 + 2(A_7 + A_8)x_1^2$
			SS = $(0, 0, x_2, x_2)$	$(0, 0, q, q)$ $(q, q, 0, 0)$	$-2\lambda_2$ $\lambda_1 + (2A_3 + A_4)x_2^2$
$(q_1, q_1, q_2, -q_2)$	$\mathbf{D}_4$	$\gamma_{L/2}^{xy} r s_1, s_6$	LS = $(x_1, x_1, 0, 0)$	$(q, q, 0, 0)$ $(0, 0, q, -q)$	$-2\lambda_1$ $\lambda_2 + 2(A_7 - A_8)x_1^2$
			SS = $(0, 0, x_2, -x_2)$	$(0, 0, q, -q)$ $(q, q, 0, 0)$	$-2\lambda_2$ $\lambda_1 + (2A_3 - A_4)x_2^2$
$(q_1, q_2, iq_3, iq_3)$	$\mathbf{D}_2$	$s_4, \gamma_{L/2}^{xy} r s_2$	LS = $(x_1, x_1, 0, 0)$	$(q, q, 0, 0)$ $(q, -q, 0, 0)$ $(0, 0, iq, iq)$	$-2\lambda_1$ $\lambda_1(A_2 - A_1)/(A_2 + A_1)$ $\lambda_2 + 2A_7x_1^2$
			SS = $(0, 0, ix_2, ix_2)$	$(0, 0, iq, iq)$ $(q, 0, 0, 0)$ $(0, q, 0, 0)$	$-2\lambda_2$ $\lambda_1 + (2A_3 - A_4)x_2^2$ $\lambda_1 + (2A_3 + A_4)x_2^2$
$(q_1, q_1, iq_2, 0)$	$\mathbf{D}_2$	$s_6, \gamma_{L/2}^{xy} r s_2$	LS = $(x_1, x_1, 0, 0)$	$(q, q, 0, 0)$ $(0, 0, iq, 0)$	$-2\lambda_1$ $\lambda_2 + 2A_7x_1^2$
			SR = $(0, 0, ix_2, 0)$	$(0, 0, iq, 0)$ $(q, q, 0, 0)$	$-2\lambda_2$ $\lambda_1 + A_3x_2^2$

(continued on next page)

Table 8 (continued)

Subspace	Subgroup	Generators	Steady states	Eigenspaces	Eigenvalues
$(q_1, q_1, q_3, q_4)$	$D_2$	$s_2, s_6$	LS = $(x_1, x_1, 0, 0)$  SR = $(0, 0, x_2, 0)$	$(q, q, 0, 0)$ $(0, 0, q, q)$ $(0, 0, q, -q)$ $(0, 0, q, 0)$ $(0, 0, 0, q)$ $(q, q, 0, 0)$	$-2\lambda_1$ $\lambda_2 + (A_7 + A_8)x_1^2$ $\lambda_2 + (A_7 - A_8)x_1^2$ $-2\lambda_2$ $\lambda_2(A_5 - A_6)/A_5$ $\lambda_1 + A_3x_2^2$

Shown are: a typical point of a subspace (where  $q_k$  are real quantities), symmetry group, its generators, the steady states, eigenspaces, and associated eigenvalues.

Table 9

The coefficients  $\alpha_{ij}$  and  $\beta_{ij}$  in Eqs. (15) and (16) that determine the coefficients  $A_i$  and  $\lambda_i$  of the normal form Eq. (12)

$\beta_{ij}$	$\beta_{ij}$		$\alpha_{ij}$	$\alpha_{ij}$		
	$j = 1$	$j = 2$		$j = 1$	$j = 2$	$j = 3$
$i = 1$	3.1551	0.01949	$i = 1$	0	0	-0.125
$i = 2$	-4.2921	0.02456	$i = 2$	-0.03207	-0.01843	-0.18081
			$i = 3$	0.02281	0.13589	-0.1744
			$i = 4$	-0.08110	-0.3240	-0.1441
			$i = 5$	0	0	-0.125
			$i = 6$	-0.03108	-0.01958	-0.17434
			$i = 7$	-0.1954	-0.2513	-0.2667
			$i = 8$	0.1314	0.2237	-0.1096

We produce gyrant bifurcation diagrams that show the bifurcating branches on varying parameters around a small circle in the  $(k, R)$  plane that encloses the mode interaction. These are found by taking parameters  $\theta$  and  $r$  that determine the growth rates of the primary modes

$$\lambda_1 = r \cos \theta, \quad \lambda_2 = r \sin \theta \quad (17)$$

and investigating the behavior of Eq. (12) with coefficients as in Eqs. (15) and (16) determined by center manifold reduction. The cubic truncation the dynamics does not qualitatively depend on  $r$  as  $r$  can be scaled to be unity by a change in timescale.

Fig. 4 gives some bifurcation diagrams calculated in this way for a range of Prandtl numbers, where the locations of the labelled bifurcations are listed in Table 10 and  $\theta$  increases from  $-\pi/2$  at 1 to  $\pi$  at 33. Solid single lines correspond to relative equilibria that are stable if the lines are bold. Dashed lines correspond to periodic solutions that are similarly stable if the lines are bold. Wavy lines denote chaotic attractors. Double lines indicate that there are robust heteroclinic networks that exist in this region; these correspond to attractors if the lines are bold. The double lines start and end at steady bifurcations where robust cycles are created. However they do not indicate all the steady branches and bifurcations involved in the network.

For  $P = 1$  we observe the following sequence of attractors on increasing  $\theta$ . Referring to the numbered bifurcations in Fig. 4(a) up to point 1 the trivial solution is stable. At 1 (corresponding to  $\lambda_1 = 0$  and  $\lambda_2 < 0$ ) there is bifurcation to stable LR. These persist up to 17 where there is a bifurcation to RC with no nearby stable states. In the interval 17–20 the only attractor is a robust heteroclinic attractor that we describe in detail in Section 4.3. At 20 there is a subcritical Hopf bifurcation that stabilizes WR2 and that apparently destroys the stable heteroclinic attractor. The branch of WR2 is stable to 26 where it branches from and stabilizes the SR state. The latter finally disappears at point 33 (corresponding to  $\lambda_2 = 0$  and  $\lambda_1 < 0$ ).

For  $P = 0.5$  Fig. 4(b) shows a similar sequence of bifurcations as for  $P = 1$  except that the ordering and criticality of some of the steady bifurcations has changed. In addition there is a limit point 34 on the branch of subcritically branching periodic solutions from WR2 at 20. This gives rise to bistability of the WR2 solution with large amplitude periodic orbits in the interval from 20 to 34. These large amplitude periodic orbits form the only attractors for 20 to 35. As we move from 35 down to 36 there is a complicated sequence of bifurcations of periodic orbits and chaotic attractors that may be evidence of structural instability in this region. At the end of this sequence of bifurcations there is an attracting heteroclinic network between 17 and 36.

For  $P = 0.3$  and 0.1 (Fig. 4(c) and 4(d) respectively) the heteroclinic network is attracting up to 25 where the last cyclic connections are destroyed by bifurcation from LR to WR1. In both cases there is bistability of periodic solutions and WR2 in the region from 35 to 34 and a complicated sequence of bifurcations including period doubling and symmetry breaking of periodic orbits between 25 and 34. The main difference between the cases  $P = 0.3$  and  $P = 0.1$  is that the bifurcations 17 and 24 change order meaning that the region of existence of robust heteroclinic cycles splits into two intervals for  $P = 0.1$ . After destruction of the heteroclinic cycle at 25 there are highly intermittent chaotic attractors between 25 and 37. An example of such an attractor is shown in Fig. 5 for  $P = 0.1$  and  $\theta = 1.58$ .

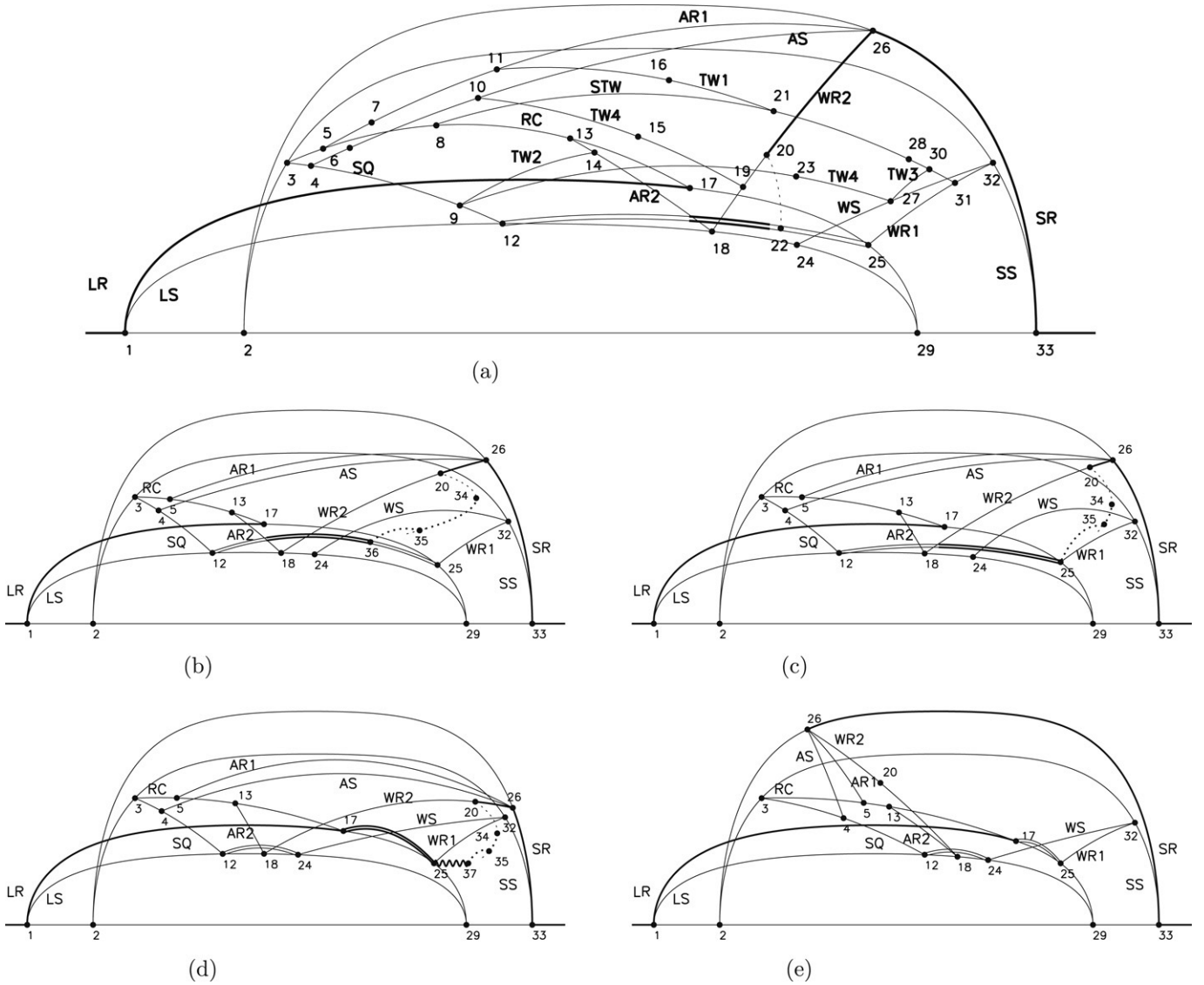


Fig. 4. Bifurcation diagrams for the reduced normal form equations for a range of Prandtl numbers; (a)  $P = 1$ , (b)  $P = 0.5$ , (c)  $P = 0.3$ , (d)  $P = 0.1$ , (e)  $P = 2$ . The horizontal axis (not shown to uniform scale) shows  $\theta$  varying from  $-\pi/2$  (labelled 1) to  $\pi$  (labelled 33). Only one representative of each branch is illustrated, and the vertical axis represents a solution norm that is also not to scale. All primary and secondary branches along with selected tertiary branches are shown. The only periodic branches shown are those bifurcating from stable states.

Finally for  $P = 2$  Fig. 4(e) shows the dynamical complexity is reduced for the attractors; there is simply bistability of LR and SR of the whole region from 26 to 17 and apparently no other attractors. There are still robust heteroclinic cycles from 12 to 24 and from 17 to 25 but they are not attracting.

#### 4.2. Bifurcations for the reduced system on varying $P$

The main (primary and secondary) bifurcations of the normal form (12) with coefficients (15), (16) and (17) are shown in Fig. 6. This illustrates the variation of the bifurcation points in Fig. 4 with  $P$ . Tertiary and Hopf bifurcations are not shown in this diagram.

To the left of the line 17 there are stable LR solutions while to the right of 26 up the line 33 there are stable SR solutions. The attracting heteroclinic cycles exist within the region enclosed by 17, 26 and  $P = 0$ . Tables 1 and 3 imply that lines 17 and 26 intersect at  $P_c$  such that

$$A_3(A_7 + A_8) = A_1A_5.$$

Substituting in Eq. (16) with coefficient values listed in Table 9 and solving the equation for  $P$  numerically we obtain  $P_c \approx 1.118$ . For  $P > P_c$  there is an interval of  $\theta$  where stable LR and SR coexist; for any  $\theta$  at least one stable steady state is always present. This implies that the heteroclinic network of the type considered in Section 4.3 (or its subcycle) cannot be an attractor or a part of an attractor for  $P > P_c$ . To see this, suppose that a heteroclinic attractor of the type considered in 4.3 exists in the system. For

Table 10

This table gives the locations of the bifurcations shown in Fig. 4 on increasing  $\theta$  from left to right for a small circuit around the mode interaction at  $(k_m, R_m)$

$P = 1$												
	1	2	3	4	5	6	7	8	9	10	11	12
$\theta$	$-\pi/2$	0	0.5425	0.6609	0.7078	0.8524	0.8845	1.019	1.057	1.127	1.136	1.2067
	13	14	15	16	17	18	19	20	21	22	23	24
$\theta$	1.2240	1.262	1.264	1.279	1.3095	1.3259	1.330	1.3444	1.352	1.353	1.372	1.3870
	25	26	27	28	29	30	31	32	33			
$\theta$	1.4411	1.4458	1.511	1.522	$\pi/2$	1.571	1.666	2.547	$\pi$			
$P = 0.5$												
	1	2	3	4	5	12	13	17	18	24		
$\theta$	$-\pi/2$	0	0.559	0.670	0.687	1.240	1.306	1.390	1.420	1.473		
	36	35	25	20	29	34	26	32	33			
$\theta$	1.500	1.508	1.519	1.547	$\pi/2$	1.646	2.557	2.842	$\pi$			
$P = 0.3$												
	1	2	3	4	5	12	13	18	17	24		
$\theta$	$-\pi/2$	0	0.590	0.703	0.727	1.272	1.379	1.460	1.465	1.503		
	25	29	35	20	34	26	32	33				
$\theta$	1.548	$\pi/2$	1.602	1.625	1.76	2.911	2.923	$\pi$				
$P = 0.1$												
	1	2	3	4	5	12	13	18	24	17		
$\theta$	$-\pi/2$	0	0.668	0.803	0.842	1.313	1.464	1.484	1.522	1.553		
	25	29	37	20	35	34	32	26	33			
$\theta$	1.567	$\pi/2$	1.645	1.647	1.660	1.85	2.948	3.106	$\pi$			
$P = 2$												
	1	2	3	26	4	5	20	13	12	18	24	17
$\theta$	$-\pi/2$	0	0.54	0.89	0.92	0.96	1.13	1.18	1.20	1.23	1.24	1.28
	25	29	32	33								
$\theta$	1.32	$\pi/2$	1.95	$\pi$								

The labels are sequential for  $P = 1$  but change ordering for different values of  $P$ .

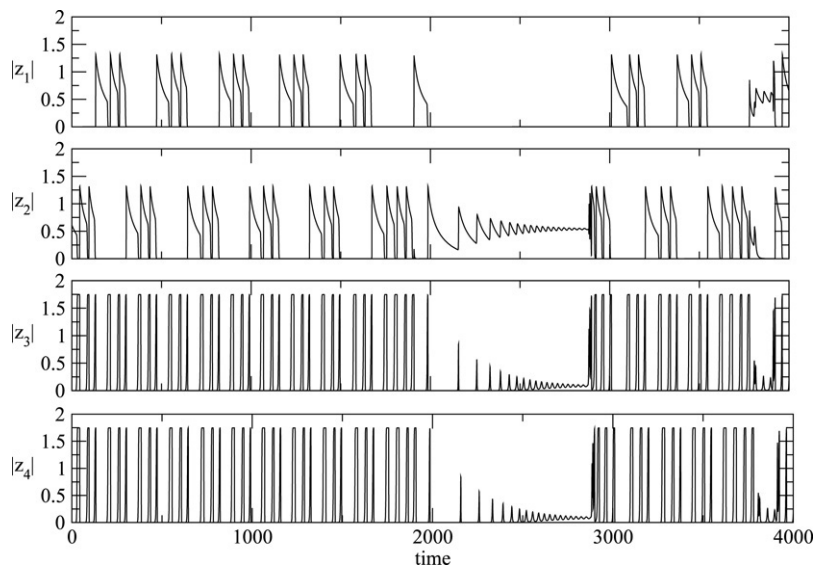


Fig. 5. Example of a chaotic attractor in the system for  $P = 0.1$  and  $\theta = 1.58$ . For  $t < 2000$  the trajectory appears to be on a periodic orbit that is close to a heteroclinic cycle, while for  $2000 < t < 3000$  there is a transition to WR2 after which (for  $2900 < t < 3000$ ) it returns to the orbit. For  $k = 1.84$ , employed in numerical investigation of convective attractors, the Rayleigh number corresponding to  $\theta = 1.58$  is  $R = 687.0$ .

$P > P_c$  at least one of SR or LR is stable. Let it be SR. Hence, SR does not belong to the heteroclinic attractor. Hence, SS belongs to the attractor. (Any subcycle involves either SR or SS.) A connection from SS to SR exists for all  $P$ , and a trajectory close to the assumed attractor finally will be attracted by the stable SR.

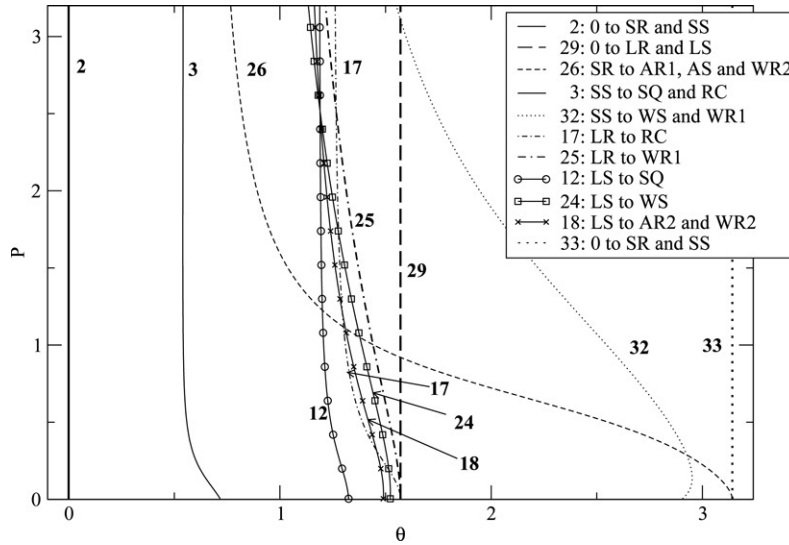


Fig. 6. Two-parameter bifurcation diagram showing the location of the primary and secondary bifurcations for a range of  $\theta$  and  $P$ . The numbering is the same as on Fig. 4. Note that the bifurcation number 1 is not shown because it is to the left of this diagram at  $\theta = -\pi/2$ .

The directions of branching and stability of bifurcating solutions in bifurcation of SR are different for different  $P$ . Appendix A demonstrates that bifurcation from SR gives three bifurcating branches. Only one of branches can be stable, and that only if all three bifurcate supercritically, the two remaining branches being unstable. Moreover the stable one has the largest amplitude. The steady state WR2 bifurcates supercritically for  $P < P_r$ , where  $P_r$  is the value for which the lines marked 26 and 18 on Fig. 6 intersect.  $P_r$  is a root of the equation

$$2A_3A_7 = A_5(A_1 + A_2).$$

Substituting here Eq. (16) with the coefficient values listed in Table 9 and solving the resultant equation numerically we obtain  $P_r \approx 1.110$ . We have checked that for  $P < P_r$  the steady state WR2 has the largest amplitude (amplitudes were calculated from Tables 3 and 9) and two other steady states bifurcate supercritically. Therefore, for  $P < P_r$  stable WR2 bifurcate from SR, and for  $P > P_r$  no stable branches bifurcate from it.

We remark that there are codimension 2 bifurcation points at all crossings of lines in the  $(\theta, P)$  plane. These are typically degenerate for the cubic truncation of the normal form; for example there is a vertical branch of WR2 on crossing of the lines 18 and 26 that can only be resolved by including fifth-order terms in Eq. (12).

### 4.3. Heteroclinic attractors for $P = 1$

We study the heteroclinic attractors in the case  $P = 1$  in more detail, for parameters in the interval between 17 and 20 in Fig. 4(a).

For the sub-interval between 19 and 20 the attractor is not a conventional type of heteroclinic cycle but also includes connections from within the cycle to a subcycle; this means that the network has depth 2 in the terminology of [1]. As such this the first example of a depth 2 cycle in a fluid dynamical system.

Fig. 7 schematically illustrates the structures of attractor for parameters in this range as far as we have been able to determine. On increasing  $\theta$  the first bifurcation at 17 creates the  $LR \rightarrow SS \rightarrow LR$  cycle at disappearance of the branch of RC. The full dynamics of all connections in the interval between 17 and 18 is not clear but there are robust connections from AS and AR1 to the cycle between LR and SS. Between 18 and 20 there is a connection from WR2 to the cycle that affects the dynamics also for nearby  $\theta$  as shown in Fig. 8. This figure shows the evolution of amplitudes of modes  $|z_i|$  for a randomly chosen initial condition for  $P = 1$  and  $\theta = 1.325$ . After an initial slowing down oscillation between LR and SS states the trajectory takes an alternative route on the unstable manifold at approximately  $t = 1000$  that takes it close to SR, then AR1 and at approximately  $t = 3300$  towards a state near where WR2 is created. The process then repeats by approaching the LR–SS cycle.

## 5. Numerical simulations of convective attractors

In this section we present some results of numerical investigation of attractors of Boussinesq convection equations (1)–(4). Computations have been performed using the standard pseudospectral methods and a fourth-order Runge–Kutta scheme for integration in time (see details in [15]) for  $P = 0.1, 0.3, 0.5, 1$  and  $2$ ,  $\delta = \pm 0.01k_m$  (i.e.  $k = 1.84$  and  $1.88$ ) and  $R$  increasing from 0. A small value of  $\delta$  has been chosen so that the third-order truncated normal form can be expected to be valid.

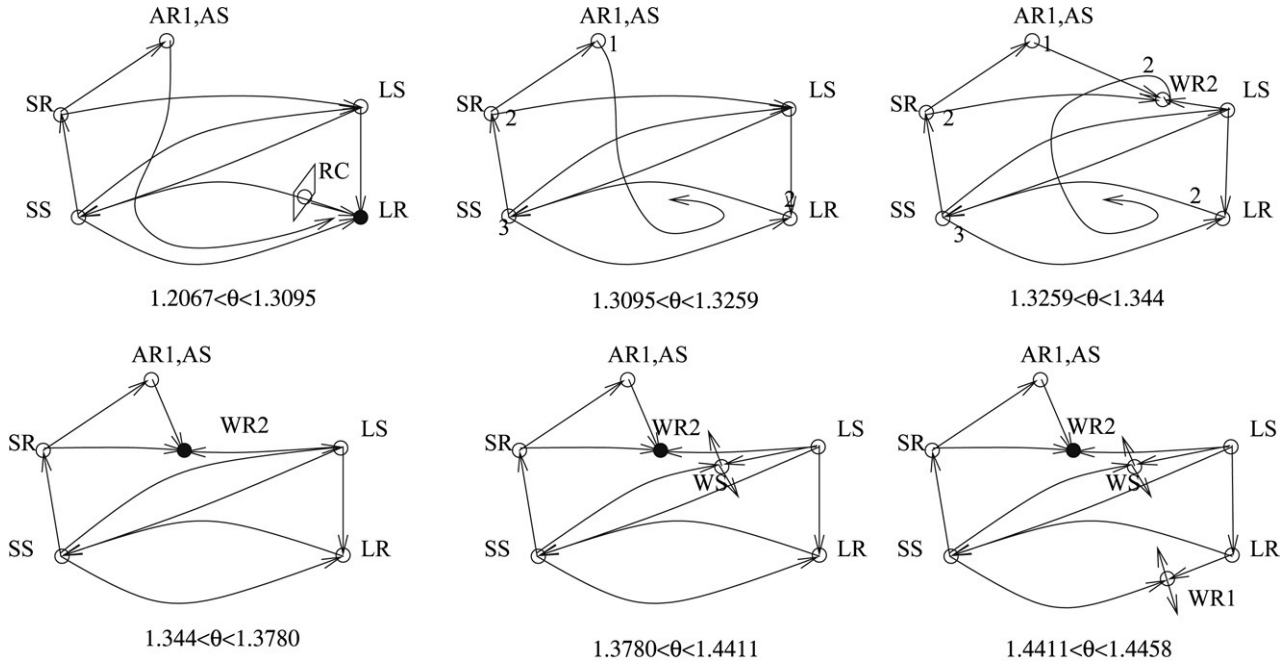


Fig. 7. Schematic illustration of connections between different symmetry types for  $P = 1$  between parameters near 18 and 25 of Fig. 4(a). Open circles indicate saddles, filled circles are sinks. The size of the unstable manifold (ignoring group orbit directions) is indicated as a number next to that state. Note that for  $1.2067 < \theta < 1.3095$  from 12 to 17, LR is the only attractor. For  $1.3095 < \theta < 1.344$  from 17 to 20 the only attractor is a network involving all states and including a connection to the subcycle including LR and SS. The bifurcation at  $\theta = 1.344, 20$ , is a subcritical Hopf bifurcation that stabilizes the WR2 solution. For  $1.344 < \theta < 1.3780$  from 20 to 25 there is still a heteroclinic cycle between LR and SS states but typical orbits near this are transients to the WR2 state.

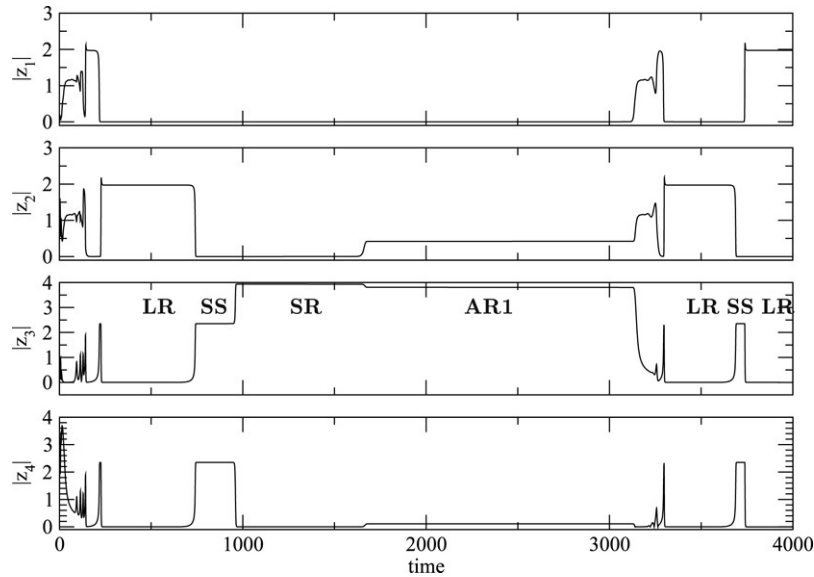


Fig. 8. Time series showing a typical trajectory approaching a depth 2 heteroclinic network for  $P = 1$  and  $\theta = 1.325$ . Note the approach to a cycle between LR and SS states is interrupted by the trajectory choosing the unstable manifold towards an AR1 and then a WR2 state. For  $t > 3300$  it heads towards LS before showing oscillatory growth near where WR2 appears for  $\theta > 1.3259$ .

Attractors found in numerical simulations are listed in Table 11, where intervals of existence of attractors are given in terms of both  $R$  and  $\theta$ , where  $\theta$  is calculated from  $R$  using Eq. (14), (15) and (17):

$$\tan \theta = \frac{\lambda_2}{\lambda_1} = \frac{\beta_{21} + \beta_{22}(R - R_m)/\delta}{\beta_{11} + \beta_{12}(R - R_m)/\delta}$$

and hence a straight line on the  $(k, R)$  plane corresponds to each value of  $\theta$ . Therefore,  $\theta \rightarrow \theta_\infty = \arctan(\beta_{22}/\beta_{12}) \approx 0.900$  as  $R \rightarrow \infty$  and on the diagrams of Fig. 4 the part  $\theta < \theta_\infty$  corresponds to  $\delta > 0$  and the part  $\theta > \theta_\infty$  to  $\delta < 0$ .

Table 11  
Attractors found in numerical simulations of convective flows

$P$	$\delta$	Type of attractor	Interval of existence ( $R$ )	Interval of existence ( $\theta$ )	
2	$-0.01k_m$	$S_0$	$R \leq 681.2$	$\theta \geq 3.1287$	
		SR	$681.3 \leq R \leq 736.1$	$0.9549 \leq \theta \leq 3.1068$	
		LR	$690.1 \leq R \leq 2200$	$0.9018 \leq \theta \leq 1.3104$	
		$\widetilde{TW}$	$R \geq 2300$	$\theta \leq 0.9017$	
	$0.01k_m$	$S_0$	$R \leq 681.0$	$\theta \leq -1.5695$	
		LR	$681.1 \leq R \leq 2300$	$-1.5575 \leq \theta \leq 0.8979$	
1	$-0.01k_m$	$S_0$	$R \leq 681.2$	$\theta \geq 3.1287$	
		SR	$681.3 \leq R \leq 687.9$	$1.4762 \leq \theta \leq 3.1068$	
		WR2	$688 \leq R \leq 689.8$	$1.3275 \leq \theta \leq 1.4661$	
		Periodic (heteroclinic)	$688.9 \leq R \leq 690.2$	$1.3049 \leq \theta \leq 1.3879$	
		LR	$690.3 \leq R \leq 1100$	$0.9069 \leq \theta \leq 1.2996$	
		$\widetilde{TW}$	$R \geq 1200$	$\theta \leq 0.9055$	
	$0.01k_m$	$S_0$	$R \leq 681.0$	$\theta \leq -1.5695$	
		LR	$681.1 \leq R \leq 1100$	$-1.5575 \leq \theta \leq 0.8920$	
		$\widetilde{TW}$	$R \geq 1200$	$\theta \geq 0.8935$	
	0.5	$-0.01k_m$	$S_0$	$R \leq 681.2$	$\theta \geq 3.1287$
			SR	$681.3 \leq R \leq 683.2$	$2.5534 \leq \theta \leq 3.1068$
			WR2	$683.3 \leq R \leq 687.1$	$1.5697 \leq \theta \leq 2.5190$
Periodic			$686.6 \leq R \leq 687.6$	$1.5084 \leq \theta \leq 1.6421$	
Chaotic (heteroclinic)			$687.7 \leq R \leq 688.9$	$1.3879 \leq \theta \leq 1.4973$	
LR			$689 \leq R \leq 800$	$0.9248 \leq \theta \leq 1.3804$	
$0.01k_m$		$S_0$	$R \leq 681.0$	$\theta \leq -1.5695$	
		LR	$681.1 \leq R \leq 780$	$-1.5575 \leq \theta \leq 0.8653$	
		$\widetilde{TW}$	$R \geq 790$	$\theta \geq 0.8686$	
0.3		$-0.01k_m$	$S_0$	$R \leq 681.2$	$\theta \geq 3.1287$
			SR	$681.3 \leq R \leq 682.1$	$2.9038 \leq \theta \leq 3.1068$
			WR2	$682.2 \leq R \leq 686.4$	$1.6748 \leq \theta \leq 2.8750$
	Periodic		$685.9 \leq R \leq 687.4$	$1.5317 \leq \theta \leq 1.7669$	
	Chaotic (heteroclinic)		$687.5 \leq R \leq 688.1$	$1.4563 \leq \theta \leq 1.5199$	
	LR		$688.2 \leq R \leq 720$	$0.9790 \leq \theta \leq 1.4468$	
	$0.01k_m$	$S_0$	$R \leq 681.0$	$\theta \leq -1.5695$	
		LR	$681.1 \leq R \leq 710$	$-1.5575 \leq \theta \leq 0.7687$	
		$\widetilde{PO}$	$R \geq 720$	$\theta \geq 0.8061$	
	0.1	$-0.01k_m$	$S_0$	$R \leq 681.2$	$\theta \geq 3.1287$
			SR	$R = 681.3$	$\theta = 3.1068$
			WR2	$681.4 \leq R \leq 686.2$	$1.7097 \leq \theta \leq 3.0841$
Periodic			$685.7 \leq R \leq 686.7$	$1.6266 \leq \theta \leq 1.8084$	
Chaotic (heteroclinic)			$686.8 \leq R \leq 687.3$	$1.5440 \leq \theta \leq 1.6117$	
LR			$687.4 \leq R \leq 690$	$1.3159 \leq \theta \leq 1.5317$	
$0.01k_m$		$S_0$	$R \leq 681.0$	$\theta \leq -1.5695$	
		LR	$681.1 \leq R \leq 684$	$-1.5575 \leq \theta \leq -1.0009$	
		$\widetilde{PO}$	$R \geq 685$	$-0.7087$	

For  $P = 2$  for the range of  $R$  where the center manifold approximation is valid the attractors are either SR or LR, in agreement with results of Section 4.1.

For  $P = 1$  and  $\delta = -0.01k_m$  for increasing  $R$  we observe transitions from  $S_0$  to SR and to WR2. Simultaneously with the WR2, there exists another attractor, a periodic orbit of a very large period which is close to the heteroclinic cycle connecting LR and SS. On Fig. 9(a) the plateaux with  $|z_1| \neq 0$ ,  $|z_2| \neq 0$  and  $|z_3| = |z_4| \neq 0$  indicate time intervals when the shown trajectory is close to large rolls parallel to the  $y$  axis, large rolls parallel to the  $x$  axis, and to small squares, respectively. The orbit has appeared from the cycle either due to numerical inaccuracy, or perhaps for some other unknown reasons. For larger  $R$  the attractor is LR, which then bifurcates to a  $\widetilde{TW}$ , this bifurcation being outside the region of validity of the approximation. For  $\delta = 0.01k_m$ , where the approximation is valid, the attractor is LR.

For  $P = 0.5$  and  $\delta = -0.01k_m$  we also see bifurcations from  $S_0$  to SR and to WR2. In agreement with the bifurcation diagram for the eight-dimensional system, the periodic orbit bifurcating from WR2 undergoes a saddle-node bifurcation and becomes stable

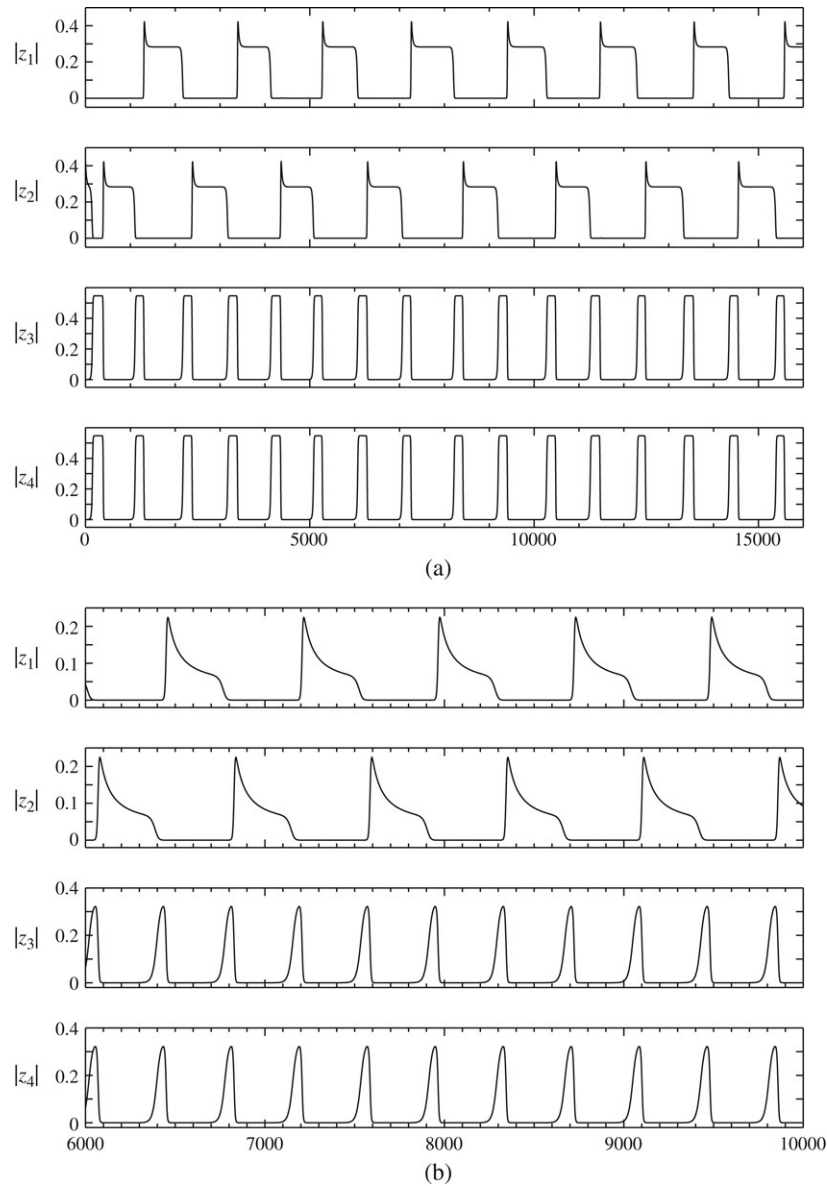


Fig. 9. Temporal evolution of the quantities  $|z_1|$ ,  $|z_2|$ ,  $|z_3|$  and  $|z_4|$  of convective attractors for  $\delta = -0.01k_m$  ( $k = 1.84$ ) and (a)  $P = 1$ ,  $R = 690$  ( $\theta = 1.3159$ ); (b)  $P = 0.5$ ,  $R = 687.5$  ( $\theta = 1.5199$ ); (c)  $P = 0.5$ ,  $R = 688.5$  ( $\theta = 1.4219$ ) and (d)  $P = 0.1$ ,  $R = 688$  ( $\theta = 1.4661$ ). (See the details in the text.) By  $|z_i|$ ,  $i = 1, 4$ , we denote projections into the basic vectors in the center eigenspace. The horizontal axis shows time.

(Fig. 9(b)). Unlike in the eight-dimensional normal form, the branch of periodic orbits ends on the heteroclinic cycle, instead of bifurcating to another orbit (note the similarity between Fig. 9(a) and (b); the trajectory visits unstable LR and SS flows on both plots, but the period of the orbit in part (b) is smaller, and it increases as  $R$  gets closer to the point of bifurcation of the orbit into the heteroclinic cycle involving LR and SS). The bifurcation value of  $R$  is the lower end of the interval of chaotic heteroclinic behavior, where trajectories jump between LR and SS steady states. In each run the time spent near each of the steady state changes randomly, unlike for  $P = 1$  (Fig. 9(a)). We also observe occasional transitions  $SS \rightarrow LS \rightarrow SS$  (e.g. the trajectory shown on Fig. 9(c) at  $t \approx 8500$  is close to the LS steady state, other plateaux correspond to the LR or SS steady states), i.e. another cycle predicted by the theory persists in the temporal evolution.

For  $P = 0.3$  and for  $P = 0.1$  attractors are the same as for  $P = 0.5$ . For  $P = 0.1$  the heteroclinic cycle connecting SS and LS is always unstable, but it is visible as a transient in some runs for  $687.8 \leq R \leq 688.1$  (in Fig. 9(d) in the interval  $1000 \leq t \leq 6500$ , when  $|z_1|$  and  $|z_2|$  are small the trajectory is close to SS, and when  $|z_3|$  and  $|z_4|$  are small to LS).

In simulations with  $\delta = \pm 0.05k_m$  and  $P = 1$  the same sequence of bifurcations as for  $\delta = \pm 0.01k_m$  has been observed. In [16] numerical investigation of convective attractors was carried out with  $L = 4$  (i.e.  $\delta = -0.16k_m$ ) and  $P = 6.8, 1$  and  $0.3$ . Some of the observed bifurcations are the same as in the reduced system considered here, but several are different, e.g. for  $P = 1$  and  $0.3$  the bifurcation from WR2 is supercritical.

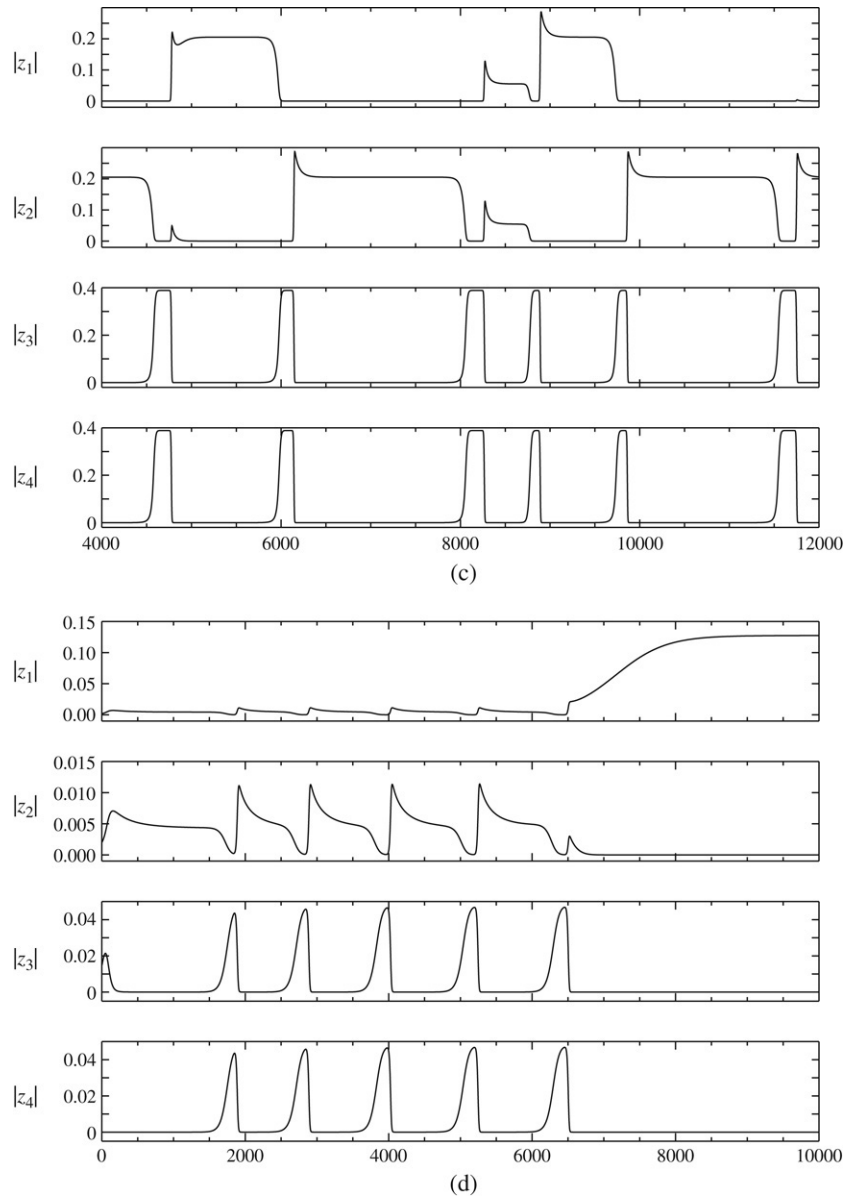


Fig. 9. (continued)

### 6. Comparison of bifurcations in the original and reduced systems

Critical values of  $\theta$  for the reduced system and for the original convective system are compared in Table 12 for the bifurcations which are identical in the two systems. Since for the convective system results are obtained numerically, information about bifurcations of attractors only is available, and only brackets for critical  $\theta$ 's are known.

The critical values of  $\theta$  (see Table 12) are similar for the original and reduced systems. Attractors (for  $R$  such that the center manifold approximation is valid) are also similar, except where heteroclinic attractors are present. In such cases the numerics may not shadow the true system dynamics. This is because numerical noise (including rounding errors) can cause the heteroclinic attractor to appear as a long period orbit that moves very close to states with different symmetries.

In the convective simulations analogues of the following attractors of the reduced system were not found: for  $P = 0.5$  periodic orbits existing between bifurcations 36 and 35; for  $P = 0.3$  periodic orbits existing between 25 and 35; for  $P = 0.1$  the irregular chaotic attractor illustrated in Fig. 5 between 25 and 37 is replaced by a more regular heteroclinic behavior, similar to the one shown in Fig. 9(a) and (c).

Hence many of the more subtle effects due to heteroclinic connections within attractors are not well reproduced numerically. Indeed numerical integration of the original system can be viewed as an ideal system perturbed by low amplitude noise of numerical origin. It is known [21] that additive noise in a system with heteroclinic attractors typically produces approximately periodic

Table 12

Comparison of critical values of  $\theta$ 's for bifurcation occurring in the original convection problem and the reduced system

$P$	Number of bifurcation	$\theta_c$ (reduced system)	$\theta_c$ (convection)
2	1	$-\pi/2$	(-1.5695, -1.5575)
	26	0.89	(0.9548, 0.9549)
	17	1.28	(1.3104, 1.3159)
	33	$\pi$	(3.1068, 3.1287)
1	1	$-\pi/2$	(-1.5695, -1.5575)
	17	1.3095	(1.2996, 1.3049)
	20	1.330	(1.3216, 1.3275)
	26	1.4458	(1.4661, 1.4762)
0.5	33	$\pi$	(3.1068, 3.1287)
	1	$-\pi/2$	(-1.5695, -1.5575)
	17	1.390	(1.3804, 1.3879)
	36	1.500	(1.4973, 1.5084)
	20	1.547	(1.5566, 1.5697)
	34	1.646	(1.6421, 1.6581)
	26	2.557	(2.5190, 2.5534)
0.3	33	$\pi$	(3.1068, 3.1287)
	1	$-\pi/2$	(-1.5695, -1.5575)
	17	1.465	(1.4468, 1.4563)
	25	1.548	(1.5199, 1.5317)
	20	1.625	(1.6521, 1.6748)
	34	1.76	(1.7669, 1.7873)
	26	2.911	(2.8750, 2.9038)
0.1	33	$\pi$	(3.1068, 3.1287)
	1	$-\pi/2$	(-1.5695, -1.5575)
	17	1.553	(1.5337, 1.5440)
	25	1.567	(1.6117, 1.6226)
	20	1.647	(1.6920, 1.7097)
	34	1.85	(1.8084, 1.8303)
	26	3.106	(3.0841, 3.1068)
33	$\pi$	(3.1068, 3.1287)	

behavior and this is what we often observe. Similarly, an orbit of a very long period instead of a theoretically predicted heteroclinic cycle related to the 1:2 mode interaction was observed in non-Boussinesq convection by Mercader et al. [13]. They suggested that higher modes present in the PDE's could possibly prevent formation of the structurally stable heteroclinic cycle with the result that a long periodic orbit was present instead.

Center manifold approximation is not valid for the  $R$ 's for which bifurcations to  $\widetilde{\text{TW}}$  and  $\widetilde{\text{PO}}$  (see Table 11) take place ( $\widetilde{\text{TW}}$  and  $\widetilde{\text{PO}}$  are periodic in time, and in the system (12) no bifurcations from rolls to time-periodic flows are possible; see Table 3). The range of validity of the approximation decreases with  $P$ , for the considered  $|\delta| = 0.01k_m$  it is  $(R - R_c) \sim 3.5R_c$  for  $P = 2$  and  $(R - R_c) \sim 0.005R_c$  for  $P = 0.01$ .

## 7. Conclusions

We have analyzed bifurcations of steady states and travelling waves emerging in the third-order normal form invariant under the considered action of  $\mathbf{D}_4 \times \mathbf{T}^2 \times \mathbf{Z}_2$  for arbitrary normal form coefficients. We have derived sufficient conditions for existence in the system of up to seven types of distinct (unrelated by symmetries) heteroclinic connections, which can form a complex network. The results have been applied to Boussinesq convection in a plane layer with stress-free boundaries and a square lattice periodicity in horizontal directions. They can be applied to other planar systems, e.g. to Boussinesq convection with other boundary conditions (as long as they are the same on upper and lower boundaries) or to systems in chemistry and biology.

For a complete study of bifurcations of steady states in the system with the symmetry group  $\mathbf{D}_4 \times \mathbf{T}^2 \times \mathbf{Z}_2$  some of the fifth-order terms should be included into the normal form. They become important if  $A_1 = A_2$  or  $A_5 = A_6$ . However, in Boussinesq convection with both stress-free or both rigid boundaries, these coefficients are unequal and thus the fifth-order terms are irrelevant. In Boussinesq binary-fluid convection and magnetoconvection (with the same symmetry groups) with stress-free boundaries these pairs of normal form coefficients are never equal [19,4] as well.

For several values of the Prandtl number, comparison has been carried out between attractors of the reduced system and attractors found by numerical simulation of equations for convection. The attractors are similar in the two systems, except for some heteroclinic attractors; this is apparently the effect of numerical noise which is introduced into the convection system [21]. Critical parameter values also turn out to be close as demonstrated in Table 12. The interval where the center manifold approximation is

valid varies from  $R - R_c < 3.5R_c$  at  $P = 2$  to  $R - R_c < 0.005R_c$  at  $P = 0.1$ . For Prandtl number close to  $P = 1$  and below, the reduced system possesses complex heteroclinic networks. We observe some highly nontrivial intermittent spatio-temporal behavior in the form of heteroclinic cycles of depth 2.

Natural questions arising from this study are what happens if symmetries of the system are slightly broken: a square periodicity cell is changed to a rectangular or rhombic cell, weak rotation or weak non-Boussinesq effects are added. In the presence of weak symmetry breaking, heteroclinic attractors are typically destroyed giving rise to temporally periodic intermittent oscillations. It would be interesting to understand the influence of noise on the attracting heteroclinic dynamics, for example that observed in Fig. 7. Preliminary investigations indicate that it appears to stabilize the cycle between SS and LR. Finally, the convective regimes that we consider can be unstable to perturbations with other spatial periods. Nonetheless our results give a good indication of minimum complexity of the spatio-temporal dynamics of planar convection.

### Acknowledgments

Part of the research of OP was carried out during visits to the University of Exeter, in February–May 2006. We are grateful to the Royal Society for the support of the visit. Some numerical results were obtained using computational facilities provided by the program “Simulations Interactives et Visualisation en Géophysique, Astronomie, Mathématique et Mécanique (SIGAMM)” at Observatoire de la Côte d’Azur, France. The work of OP at the Observatoire de la Côte d’Azur was supported by the French Ministry of Education.

### Appendix A. Steady state bifurcation with the $\mathbf{D}_2 \times \mathbf{T} \times \mathbf{Z}_4$ symmetry group

We apply theory and methods of [8] to find branches of steady states emerging in a steady state bifurcation with this symmetry group. Consider the action of  $\mathbf{D}_2 \times \mathbf{T} \times \mathbf{Z}_4$  on  $\mathbf{C}^2$  generated by

$$\begin{aligned} h_1(=s_2) &: (w_1, w_2) \rightarrow (\bar{w}_1, \bar{w}_2), \\ h_2(=s_6) &: (w_1, w_2) \rightarrow (w_2, w_1), \\ \psi_\alpha(=\gamma_\alpha^{x,-y}) &: (w_1, w_2) \rightarrow (e^{2\pi i\alpha/L} w_1, e^{-2\pi i\alpha/L} w_2), \\ h_3(=\gamma_{L/4}^{xy}) &: (w_1, w_2) \rightarrow (-iw_1, -iw_2). \end{aligned}$$

The third-order dynamical system commuting with the group action (derived following the procedure described in [17]) is

$$\begin{aligned} \dot{w}_1 &= \mu w_1 + w_1(B_1|w_1|^2 + B_2|w_2|^2) + B_3\bar{w}_1(\bar{w}_2)^2, \\ \dot{w}_2 &= \mu w_2 + w_2(B_1|w_2|^2 + B_2|w_1|^2) + B_3\bar{w}_2(\bar{w}_1)^2. \end{aligned} \tag{18}$$

One-dimensional fixed point subspaces are:  $(x, x)$  (the isotropy subgroup is  $\mathbf{D}_2$  generated by  $h_1$  and  $h_2$ ),  $(x, ix)$  (the isotropy subgroup is  $\mathbf{D}_2$  generated by  $\psi_{L/4}h_2$  and  $h_1h_2h_3$ ),  $(x, 0)$  (the isotropy subgroup is  $\mathbf{D}_2$  generated by  $h_1$  and  $h_3\psi_{L/4}$ ). Equations for amplitudes of steady states bifurcating from  $(w_1, w_2) = \mathbf{0}$  at  $\mu = 0$  in the respective subspaces are

$$\begin{aligned} (x, x) &: \mu + (B_1 + B_2 + B_3)x^2 = 0, \\ (x, ix) &: \mu + (B_1 + B_2 - B_3)x^2 = 0, \\ (x, 0) &: \mu + B_1x^2 = 0. \end{aligned} \tag{19}$$

Stability of a steady state is determined by eigenvalues of Eq. (18) linearized in the vicinity of the steady state, which are

steady state	eigenspace	eigenvalue
$(x, x)$	$(q, q)$	$2(B_1 + B_2 + B_3)x^2$
	$(q, -q)$	$2(B_1 - B_2 - B_3)x^2$
	$(iq, iq)$	$-4B_3x^2$
	$(iq, -iq)$	0
$(x, ix)$	$(q, iq)$	$2(B_1 + B_2 - B_3)x^2$
	$(q, -iq)$	$2(B_1 - B_2 + B_3)x^2$
	$(iq, -q)$	$4B_3x^2$
	$(iq, q)$	0
$(x, 0)$	$(q, 0)$	$2B_1x^2$
	$(0, q)$	$(-B_1 + B_2 + B_3)x^2$
	$(0, iq)$	$(-B_1 + B_2 - B_3)x^2$
	$(iq, 0)$	0

(20)

Comparison of Eq. (19) with Eq. (20) implies that just one branch is stable if all three bifurcate supercritically; the stable branch is the one with the largest amplitude. If there is a branch bifurcating subcritically, all three are unstable.

## Appendix B. Bifurcations to travelling waves

In this subsection we consider examples of a steady state bifurcation to travelling waves (which are also called relative equilibria in [11]), a pattern which is steady in a comoving reference frame and periodic in a reference frame at rest. Such bifurcation happens if the isotypic component containing the critical eigenmode also contains an eigenmode responsible for the shift along the group orbit of the bifurcating steady state (the associated eigenvalue is zero).

Expressions in the r.h.s. of Eq. (13) involve angles only in combinations:

$$\phi = 2\theta_1 - \theta_3 - \theta_4 \quad \text{and} \quad \psi = 2\theta_2 - \theta_3 + \theta_4.$$

Assuming  $r_3 \neq 0$  and  $r_4 \neq 0$ , one can rewrite the system (13) as

$$\begin{aligned} \dot{r}_1 &= r_1(\lambda_1 + A_1 r_1^2 + A_2 r_2^2 + A_3(r_3^2 + r_4^2)) + A_4 r_1 r_3 r_4 \cos \phi \\ \dot{r}_2 &= r_2(\lambda_1 + A_1 r_1^2 + A_2 r_1^2 + A_3(r_3^2 + r_4^2)) + A_4 r_2 r_3 r_4 \cos \psi \\ \dot{r}_3 &= r_3(\lambda_2 + A_5 r_3^2 + A_6 r_4^2 + A_7(r_1^2 + r_2^2)) + A_8(r_2^2 r_4 \cos \psi + r_1^2 r_4 \cos \phi) \\ \dot{r}_4 &= r_4(\lambda_2 + A_5 r_4^2 + A_6 r_3^2 + A_7(r_1^2 + r_2^2)) + A_8(r_2^2 r_3 \cos \psi + r_1^2 r_3 \cos \phi) \\ \dot{\phi} &= \sin \phi (-2A_4 r_3 r_4 - A_8 r_1^2 (r_4/r_3 + r_3/r_4)) - \sin \psi A_8 r_2^2 (r_4/r_3 - r_3/r_4) \\ \dot{\psi} &= \sin \psi (-2A_4 r_3 r_4 - A_8 r_2^2 (r_4/r_3 + r_3/r_4)) - \sin \phi A_8 r_1^2 (r_4/r_3 - r_3/r_4). \end{aligned} \quad (21)$$

The steady states of Eq. (21) with  $\phi = \psi = 0$  are true steady states of Eq. (13). Steady states with one of  $\phi$  or  $\psi$  non-vanishing are patterns drifting along the  $x$  or  $y$  direction, respectively. If  $\phi = \pm\psi \neq 0$ , the pattern is drifting along the diagonal. Finally, if  $0 \neq \phi \neq \psi \neq 0$ , there is drift in both horizontal directions.

### B.1. Bifurcation from RC

A steady state of Eq. (21) which belongs to the subspace  $(r_1, 0, r_3, r_3, \phi, 0)$  satisfies

$$\begin{aligned} \lambda_1 + A_1 r_1^2 + 2A_3 r_3^2 + A_4 r_3^2 \cos \phi &= 0, \\ \lambda_2 + (A_5 + A_6) r_3^2 + A_7 r_1^2 + A_8 + r_1^2 \cos \phi &= 0, \\ A_4 r_3^2 + A_8 r_1^2 &= 0. \end{aligned}$$

For them, both  $\phi = 0$  and  $\phi \neq 0$  are possible. Assume that the  $\lambda$ 's depend on a parameter  $Q$ . The two types of steady states coincide at a point where

$$\begin{aligned} \lambda_1(Q) + A_1 r_1^2 + 2A_3 r_3^2 + A_4 r_3^2 &= 0, \\ \lambda_2(Q) + (A_5 + A_6) r_3^2 + A_7 r_1^2 + A_8 + r_1^2 &= 0, \\ A_4 r_3^2 + A_8 r_1^2 &= 0. \end{aligned}$$

This system of three equations in three variables  $(Q, r_1, r_3)$  is, in general, solvable. The steady state with  $\phi = 0$  exists for  $Q$  both slightly larger and slightly smaller than the critical value; the steady state with  $\phi \neq 0$  exists only on one side of the critical  $Q$ , because  $\cos \phi \leq 1$ . The pattern moves along the  $x$  axis with the speed

$$\dot{\theta}_1 = A_4 r_3 r_4 \sin \phi,$$

small near the point of bifurcation.

### B.2. Bifurcation from SQ

In polar coordinates the action of the symmetry group of SQ,  $\mathbf{D}_4$ , on the subspace  $(0, 0, 0, 0, \phi, \psi)$  is generated by

$$\begin{aligned} s_1 : (\phi, \psi) &\mapsto (\psi, -\phi) \quad \text{and} \\ s_4 : (\phi, \psi) &\mapsto (\phi, -\psi). \end{aligned}$$

Therefore [8], there are two types of maximal isotropy bifurcating branches: with  $\psi = 0$  (or  $\phi = 0$ ) and  $\psi = \phi$  (or  $\psi = -\phi$ ). They are TW2 =  $(r_1, r_2, r_3, r_3, \phi, 0)$  and TW4 =  $(r_1, r_1, r_3, r_4, \phi, \phi)$ . In the normal form Eq. (21) TW4 bifurcating from SQ will have the form  $(r_1, r_1, r_3, r_3, \phi, \phi)$  (i.e.  $r_3 = r_4$ ) because the terms breaking this relation are outside the third-order truncation we are considering.

### Appendix C. Bifurcations from AS1

When calculating stability and bifurcations from tertiary branches we have determined three-dimensional isotypic components for the actions of the steady state symmetry groups. For one- and two-dimensional subspaces the study is straightforward; the case of three dimensions is more difficult. Here we demonstrate that some results on bifurcations and stability can be obtained without explicit calculation of eigenvalues, considering as an example bifurcations from AS1 =  $(x_1, ix_2, x_3, x_3)$  with the critical mode belonging to the subspace  $(q_1, iq_2, q_3, q_3)$ .

The matrix of the restriction of the linearization of (8) onto the subspace is

$$\mathcal{B} = \begin{pmatrix} 2A_1x_1^2 & 2A_2x_1x_2 & (4A_3 + 2A_4)x_1x_3 \\ 2A_2x_1x_2 & 2A_1x_1^2 & (4A_3 - 2A_4)x_2x_3 \\ 2(A_7 + A_8)x_1x_3 & 2(A_7 - A_8)x_1x_3 & 2(A_5 + A_6)x_3^2 \end{pmatrix}. \quad (22)$$

Its eigenvalues satisfy

$$\mu_1\mu_2\mu_3 = \det \mathcal{B}, \quad \mu_1 + \mu_2 + \mu_3 = \text{tr } \mathcal{B}, \quad \mu_1\mu_2 + \mu_1\mu_3 + \mu_2\mu_3 = \tilde{\mathcal{B}},$$

where by  $\tilde{\mathcal{B}}$  we denote the sum of the three second-order minors of  $\mathcal{B}$ .

The necessary and sufficient conditions for steady state bifurcations are  $\det \mathcal{B} = 0$ . Eq. (22) implies that  $\det \mathcal{B} = x_1^2x_2^2x_3^2F(\mathbf{A})$ . The values of  $x_j$ ,  $j = 1, 2, 3$ , for the steady state satisfy a linear system of equations on  $x_j^2$ , stemming from (12). By Cramers' rule, the solution of the system is

$$x_j^2 = \frac{g_j(\lambda_1, \lambda_2, \mathbf{A})}{f(\mathbf{A})}, \quad j = 1, 2, 3,$$

where  $g_j$  is linear in  $\lambda$ 's and quadratic in  $A$ 's, and  $f$  is cubic in  $A$ 's. It turns out that  $f(\mathbf{A}) = F(\mathbf{A})$ . Hence, the condition  $\det \mathcal{B} = 0$  is never satisfied and the condition  $F(\mathbf{A}) = 0$  gives a boundary of the domain where AS1 exists.

A Hopf bifurcation takes place if

$$\text{tr } \mathcal{B}\tilde{\mathcal{B}} = \det \mathcal{B}, \quad \tilde{\mathcal{B}} > 0;$$

and hence bifurcations from the steady state can be found by solving this equation simultaneously with equations for the steady state.

### Appendix D. Calculation of $\lambda_1$ and $\lambda_2$

We calculate here coefficients of the linear terms of (12) using the method that was employed in [2] and [14].

Denote by  $\mathcal{L}$  the system (1)–(4) linearized near the trivial steady state. The subspace spanned by

$$\mathbf{S}_1 = \begin{pmatrix} -\pi l^{-1} \cos \pi z \sin lx \\ 0 \\ \sin \pi z \cos lx \\ 0 \end{pmatrix}, \quad \mathbf{S}_2 = \begin{pmatrix} 0 \\ \cos \pi z \sin lx \\ 0 \\ 0 \end{pmatrix}, \quad \mathbf{S}_3 = \begin{pmatrix} 0 \\ 0 \\ 0 \\ \sin \pi z \cos lx \end{pmatrix} \quad (23)$$

is  $\mathcal{L}$ -invariant:

$$\begin{aligned} \mathcal{L}\mathbf{S}_1 &= -Pa\mathbf{S}_1 + \mathbf{S}_3, \\ \mathcal{L}\mathbf{S}_2 &= -Pa\mathbf{S}_2, \\ \mathcal{L}\mathbf{S}_3 &= PRl^2a^{-1}\mathbf{S}_1 - a\mathbf{S}_3, \end{aligned} \quad (24)$$

where  $a = l^2 + \pi^2$ . Therefore, there is an eigenvalue  $-P(l^2 + \pi^2)$  with the associated eigenvector  $\mathbf{S}_2$  and two eigenvalues

$$\Lambda_{\pm}(l, R) = \frac{1}{2}(-Pa + a) \pm D^{1/2} \quad \text{where } D = (Pa + a)^2 - 4(Pa^2 - PRl^2a^{-1}).$$

In the vicinity of  $l_0$  and  $R_0$ , such that  $\Lambda_+(l_0, R_0) = 0$ , Taylor expansion of  $\Lambda_+$  in  $\delta = l - l_0$  and  $\epsilon = R - R_0$  yields

$$\Lambda_+(l, R) = P(P + 1)^{-1}(2(\pi^2 - 2l_0^2)l_0^{-1}\delta + l_0^2a^{-2}\epsilon) + O(\epsilon^2 + \delta^2). \quad (25)$$

Substituting into Eq. (25)  $l_0 = k_m$  and  $l_0 = \sqrt{2}k_m$ , we find

$$\lambda_1 = P(P + 1)^{-1}(2(\pi^2 - 2k_m^2)k_m^{-1}\delta + k_m^2(\pi^2 + k_m^2)^{-2}\epsilon) + O(\epsilon^2 + \delta^2)$$

and

$$\lambda_2 = P(P+1)^{-1}(2(\pi^2 - 4k_m^2)k_m^{-1}\delta + 2k_m^2(\pi^2 + 2k_m^2)^{-2}\epsilon) + O(\epsilon^2 + \delta^2).$$

For  $k_m$  given by (8) these relations yield the coefficients  $\beta_{ij}$  presented in Table 9.

### Appendix E. Center manifold reduction

The center manifold is an invariant manifold tangent to  $X_c$  at  $(\mathbf{0}, R_m)$ ; standard theory [10] means that near a bifurcation the local solutions are determined by the dynamics on the center manifold. Locally it is represented as a graph of the mapping  $\psi(\mathbf{v}) : X_c \rightarrow X_h$  defined in a neighborhood of  $(\mathbf{0}, R_m)$ .

The second-order Taylor's expansion is

$$\psi(\mathbf{v}) = \sum_{j,l=1}^4 \phi_{j,l}^1 x_j x_l + \sum_{j,l=1}^4 \phi_{j,l}^2 x_j y_l + \sum_{j,l=1}^4 \phi_{j,l}^3 y_j y_l, \quad (26)$$

where  $x_j$  and  $y_l$  are components of  $(\mathbf{v}) \in X_c$  in the basis  $\{\mathbf{X}_j, \mathbf{Y}_l\}$  and  $\phi \in X_h$ .

Define

$$\mathbf{f}_1(m_1, m_2, m_3) = \begin{pmatrix} k_m m_2 \cos m_3 \pi z \sin(m_1 k_m x + m_2 k_m y) \\ -k_m m_1 \cos m_3 \pi z \sin(m_1 k_m x + m_2 k_m y) \\ 0 \\ 0 \end{pmatrix}, \quad (27)$$

$$\mathbf{f}_2(m_1, m_2, m_3) = \begin{pmatrix} -\pi k_m m_1 m_3 \cos m_3 \pi z \sin(m_1 k_m x + m_2 k_m y) \\ -\pi k_m m_2 m_3 \cos m_3 \pi z \sin(m_1 k_m x + m_2 k_m y) \\ (m_1^2 + m_2^2) k_m^2 \sin m_3 \pi z \cos(m_1 k_m x + m_2 k_m y) \\ 0 \end{pmatrix}, \quad (28)$$

$$\mathbf{f}_3(m_1, m_2, m_3) = \begin{pmatrix} 0 \\ 0 \\ 0 \\ \sin m_3 \pi z \cos(m_1 k_m x + m_2 k_m y) \end{pmatrix}. \quad (29)$$

The center manifold coefficients are

$$\begin{aligned} \phi_{1,1}^1 &= (8a_1 \pi)^{-1} \mathbf{f}_3(0, 0, 2), \\ \phi_{3,3}^1 &= (8a_2 \pi)^{-1} \mathbf{f}_3(0, 0, 2), \\ \phi_{1,2}^1 &= g_1^{-1} ((P^{-1} b_1 + b_2)(\mathbf{f}_2(1, 1, 2) + \mathbf{f}_2(1, -1, 2)) + (P^{-1} b_3 + b_4)(\mathbf{f}_3(1, 1, 2) + \mathbf{f}_3(1, -1, 2))), \\ \phi_{3,4}^1 &= g_2^{-1} ((P^{-1} b_5 + b_6)(\mathbf{f}_2(2, 0, 2) + \mathbf{f}_2(0, 2, 2)) + (P^{-1} b_7 + b_8)(\mathbf{f}_3(2, 0, 2) + \mathbf{f}_3(0, 2, 2))), \\ \phi_{1,3}^1 &= P^{-1} (c_1 \mathbf{f}_1(0, 1, 0) + c_2 \mathbf{f}_1(2, 1, 0) + c_3 \mathbf{f}_1(0, 1, 2) + c_4 \mathbf{f}_1(2, 1, 2) \\ &\quad + g_3^{-1} ((d_1 + P d_2) \mathbf{f}_2(0, 1, 2) + (d_3 + P d_4) \mathbf{f}_3(0, 1, 2)) + g_4^{-1} ((d_5 + P d_6) \mathbf{f}_2(2, 1, 2) + (d_7 + P d_8) \mathbf{f}_3(2, 1, 2))), \end{aligned}$$

where

$$\begin{aligned} a_1 &= \pi^2 + k_m^2, & a_2 &= \pi^2 + 2k_m^2, & a_3 &= 2\pi^2 + k_m^2, & a_4 &= 4\pi^2 + k_m^2, & a_5 &= 4\pi^2 + 5k_m^2, \\ b_1 &= -\pi a_1 (2k_m^2)^{-1}, & b_2 &= -R\pi (4a_1 a_3)^{-1}, & b_3 &= -\pi a_1 (2a_3)^{-1}, & b_4 &= -\pi a_3 a_1^{-1}, & b_5 &= -\pi a_2 (4k_m^2)^{-1}, \\ b_6 &= -R\pi (8a_1 a_2)^{-1}, & b_7 &= -\pi a_2 (4a_1)^{-1}, & b_8 &= -\pi 2a_1 a_2^{-1}, \\ g_1 &= 4a_3^2 - k_m^2 R a_3^{-1}, & g_2 &= 16a_1^2 - k_m^2 R a_1^{-1}, & g_3 &= a_4^2 - R k_m^2 a_4^{-1}, & g_4 &= a_5^2 - 5R k_m^2 a_5^{-1}, \\ c_1 &= \pi^2 (8k_m^4)^{-1}, & c_2 &= -\pi^2 (200k_m^4)^{-1}, & c_3 &= -\pi^2 (8k_m^2 a_4)^{-1}, & c_4 &= \pi^2 (40k_m^2 a_5)^{-1}, \\ d_1 &= -\pi (7k_m^2 + 4\pi^2) (8k_m^2)^{-1}, & d_2 &= -\pi R ((2a_2)^{-1} + 3(8a_1)^{-1}) a_4^{-1}, \\ d_3 &= -\pi (7k_m^2 + 4\pi^2) (8a_4)^{-1}, & d_4 &= -\pi a_4 ((2a_2)^{-1} + 3(8a_1)^{-1}), \\ d_5 &= -\pi a_5 (40k_m^2)^{-1}, & d_6 &= -\pi R (8a_1 a_5)^{-1}, & d_7 &= -\pi/8, & d_8 &= -\pi a_5 (8a_1)^{-1}. \end{aligned}$$

All other coefficients of Eq. (26) can be obtained from these applying symmetries of the system.

### Appendix F. Exact expressions for the normal form coefficients

$$\begin{aligned}
 A_1 &= -\frac{1}{8}P(P+1)^{-1}, \\
 A_2 &= A_1 - g_1^{-1}(P+1)^{-1} \left( P^{-1}\frac{1}{2}\pi^2 a_1 + R\pi^2 k_m^2 (a_1(2k_m^2 + 4\pi^2))^{-1} + \frac{1}{4}P\pi^2(2k_m^2 + 4\pi^2) \right), \\
 A_3 &= -P(P+1)^{-1}a_1(8a_2)^{-1} \\
 &\quad + (P+1)^{-1}k_m^2(8a_1)^{-1}(4c_1k_m^2 + 2(2\pi^2 - k_m^2)(2c_2 + c_3) + 2c_4k_m^2 + g_3^{-1}(P^{-1}d_1 + d_2)\pi(5k_m^2 - \pi^2) \\
 &\quad + g_4^{-1}(P^{-1}d_5 + d_6)\pi(7k_m^2 + 5\pi^2)) + P(P+1)^{-1}a_1(8a_2)^{-1}(2k_m^2(2c_1 - 2c_2 - c_3 + c_4) + 2\pi k_m^2 g_3^{-1}(P^{-1}d_1 + d_2) \\
 &\quad + 3\pi a_2 g_3^{-1}(P^{-1}d_3 + d_4) + 2\pi k_m^2 g_4^{-1}(P^{-1}d_5 + d_6) + \pi a_2 g_4^{-1}(P^{-1}d_7 + d_8)), \\
 A_4 &= (P+1)^{-1}k_m^2(4a_1)^{-1}(-4c_1k_m^2 - 2(2\pi^2 - k_m^2)c_3 + g_3^{-1}(P^{-1}d_1 + d_2)\pi(5k_m^2 - \pi^2)) \\
 &\quad + P(P+1)^{-1}a_1(4a_2)^{-1}(2k_m^2(-2c_1 + c_3) + 2\pi k_m^2 g_3^{-1}(P^{-1}d_1 + d_2) + 3\pi a_2 g_3^{-1}(P^{-1}d_3 + d_4)), \\
 A_5 &= A_1, \\
 A_6 &= A_5 - g_2^{-1}(P+1)^{-1} \left( P^{-1}\frac{1}{2}\pi^2 a_2 + R\pi^2 k_m^2 (a_2(2k_m^2 + 2\pi^2))^{-1} + P\pi^2(k_m^2 + \pi^2) \right), \\
 A_7 &= -P(P+1)^{-1}a_2(8a_1)^{-1} \\
 &\quad + \frac{k_m^2(-2c_1a_2 + (2k_m^2 - 3\pi^2)(2c_2 + c_3) - c_4a_2 + g_3^{-1}(P^{-1}d_1 + d_2)\pi(2k_m^2 + 5\pi^2) - g_4^{-1}(P^{-1}d_5 + d_6)\pi a_2)}{(P+1)4a_2} \\
 &\quad + \frac{a_2(k_m^2(-2c_1 + 2c_2 + c_3 - c_4) - \pi k_m^2 g_3^{-1}(P^{-1}d_1 + d_2) + 2\pi a_1 g_3^{-1}(P^{-1}d_3 + d_4) - \pi k_m^2 g_4^{-1}(P^{-1}d_5 + d_6))}{P(P+1)4a_1}, \\
 A_8 &= (P+1)^{-1}k_m^2(4a_2)^{-1}(2a_2c_1 + (3\pi^2 - 2k_m^2)c_3 + g_3^{-1}(P^{-1}d_1 + d_2)\pi(2k_m^2 + 5\pi^2)) \\
 &\quad + P(P+1)^{-1}a_2(4a_1)^{-1}(k_m^2(2c_1 - c_3) - \pi k_m^2 g_3^{-1}(P^{-1}d_1 + d_2) + 2\pi a_1 g_3^{-1}(P^{-1}d_3 + d_4)).
 \end{aligned}$$

### Appendix G. Reduction of the group action

The original system of ODEs (Eq. (12)) on  $\mathbf{C}^4$  has a continuous group symmetry  $\mathbf{T}^2$  that means that conventional path following programs fail to work. However, the system can be reduced by the two-dimensional group action as follows, so that the remaining system is nondegenerate and on  $\mathbf{C}^3$ . We write Eq. (12) as

$$\begin{aligned}
 \dot{z}_1 &= f_1 \\
 \dot{z}_2 &= f_2 \\
 \dot{z}_3 &= f_3 \\
 \dot{z}_4 &= f_3
 \end{aligned} \tag{30}$$

and then define

$$a_1 = -\frac{\Im(f_1 \bar{z}_1)}{|z_1|^2}, \quad a_2 = -\frac{\Im(f_2 \bar{z}_2)}{|z_2|^2}.$$

The modified system of equations

$$\begin{aligned}
 \dot{z}_1 &= f_1 + ia_1 z_1 \\
 \dot{z}_2 &= f_2 + ia_2 z_2 \\
 \dot{z}_3 &= f_3 + i(a_1 + a_2)z_3 \\
 \dot{z}_4 &= f_3 + i(a_1 - a_2)z_4
 \end{aligned} \tag{31}$$

has solutions that are in one-to-one correspondence with those of Eq. (30). This is because the infinitesimal action of  $(e^{i\alpha} z_1, z_2, e^{i\alpha} z_3, e^{i\alpha} z_4)$  is  $(i\dot{\alpha} z_1, 0, i\dot{\alpha} z_3, i\dot{\alpha} z_4)$  and the infinitesimal action of  $(z_1, e^{i\beta} z_2, e^{i\beta} z_3, e^{-i\beta} z_4)$  is  $(0, i\dot{\beta} z_2, i\dot{\beta} z_3, -i\dot{\beta} z_4)$ . Hence, for our choice of  $a_1$  and  $a_2$ , solutions to Eq. (31) satisfy

$$\Im(\dot{z}_1 \bar{z}_1) = 0, \quad \Im(\dot{z}_2 \bar{z}_2) = 0$$

meaning that effectively we have removed the group orbit drift from the trivial stratum of the orbit space. This means that we can set  $\Im(z_1) = \Im(z_2) = 0$  and compute all solutions within this six-dimensional section of the orbit space. Note that the equations transformed this way become a system on  $\mathbf{R}^6$  on parameterizing by  $(x_1, x_2, x_3 + iy_3, x_4 + iy_4)$ . Care needs to be taken near solutions where  $z_1$  and/or  $z_2$  are zero, as the system is singular on  $x_1 = x_2 = 0$ .

## References

- [1] P. Ashwin, M.J. Field, Heteroclinic networks in coupled cell systems, *Arch. Ration. Mech. Anal.* 148 (1999) 107–143.
- [2] P. Ashwin, O. Podvigina, Hopf bifurcation with cubic symmetry and instability of ABC flow, *Proc. Roy. Soc. London* 459 (2003) 1801–1827.
- [3] T. Chawanya, Infinitely many attractors in a game dynamics system, *Progr. Theoret. Phys.* 95 (1996) 679–684.
- [4] T. Clune, E. Knobloch, Pattern selection in three-dimensional magnetoconvection, *Physica D* 74 (1994) 151–176.
- [5] J.H.P. Dawes, The  $1:\sqrt{2}$  Hopf/steady-state mode interaction in three-dimensional magnetoconvection, *Physica D* 139 (2000) 109–136.
- [6] B. Dionne, M. Silber, A.C. Skeldon, Stability results for steady, spatially-periodic planforms, *Nonlinearity* 10 (1997) 321–354.
- [7] B. Ermentrout, *Simulating, Analyzing, and Animating Dynamical Systems: A Guide to XPPAUT for Researchers and Students*, SIAM publications, Pittsburgh, 2002.
- [8] M. Golubitsky, I.N. Stewart, D. Schaeffer, *Singularities and Groups in Bifurcation Theory volume 2*, in: *Appl. Math. Sci.*, vol. 69, Springer-Verlag, New York, 1988.
- [9] P. Hirschberg, E. Knobloch, A robust heteroclinic cycle in an  $\mathbf{O}(2) \times \mathbf{Z}_2$  steady-state mode interaction, *Nonlinearity* 11 (1998) 89–104.
- [10] G. Iooss, *Bifurcation of Maps and Applications*, North-Holland, Amsterdam, 1979.
- [11] M. Krupa, Bifurcations of relative equilibria, *SIAM J. Math. Anal.* 21 (1990) 1453–1486.
- [12] M. Krupa, Robust heteroclinic cycles, *J. Nonlinear Sci.* 7 (1997) 129–176.
- [13] I. Mercader, J. Prat, E. Knobloch, Robust heteroclinic cycles in two-dimensional Rayleigh–Bénard convection without Boussinesq symmetry, *Internat. J. Bifur. Chaos* 12 (2002) 2501–2522.
- [14] O.M. Podvigina, Application of the center manifold theorem for investigation of instability of the ABC flow, *Dyn. Syst.* 21 (2006) 191–208.
- [15] O.M. Podvigina, Magnetic field generation by convective flows in a plane layer, *Eur. Phys. J. B* 50 (2006) 639–652.
- [16] O.M. Podvigina, Magnetic field generation by convective flows in a plane layer: The dependence on the Prandtl number, *Geophys. Astrophys. Fluid Dyn.* (2007) (submitted for publication).
- [17] O.M. Podvigina, P. Ashwin, D.J. Hawker, Modelling instability of ABC flow using a mode interaction between steady and Hopf bifurcations with rotational symmetries of the cube, *Physica D* 215 (2006) 62–79.
- [18] M.R.E. Proctor, P.C. Matthews,  $\sqrt{2}:1$  Resonance in non-Boussinesq convection, *Physica D* 97 (1996) 229–241.
- [19] M. Silber, E. Knobloch, Pattern selection in steady binary-fluid convection, *Phys. Rev. A* 38 (1988) 1468–1477.
- [20] M. Silber, E. Knobloch, Hopf bifurcation on a square lattice, *Nonlinearity* 4 (1991) 1063–1107.
- [21] E. Stone, P. Holmes, Random perturbations of heteroclinic attractors, *SIAM J. Appl. Math.* 50 (1990) 726–743.
- [22] J.W. Swift, *Bifurcation and symmetry in convection*, Ph.D. Thesis, University of California, Berkeley, 1984.